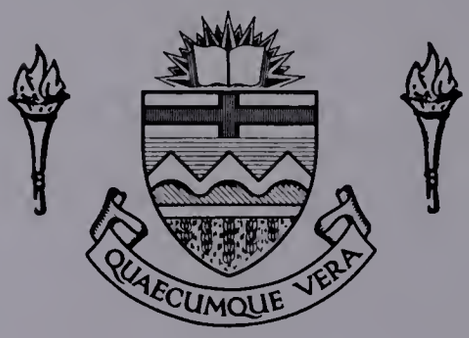

THE UNIVERSITY OF ALBERTA

THE DESIGN, CONSTRUCTION AND OPERATION OF A PHOTON-COUNTING ASTRONOMICAL PHOTOMETER

by

© GARY PEARCE FINLEY

A THESIS

SUBMITTED TO THE FACULTY OF GRADUATE STUDIES AND RESEARCH

IN PARTIAL FULFILLMENT OF THE REQUIREMENTS FOR THE DEGREE

OF MASTER OF SCIENCE

DEPARTMENT OF PHYSICS

EDMONTON, ALBERTA

FALL, 1975

ABSTRACT

The design, construction and use of a photoelectric photometer utilizing digital photon counting techniques is described. Some departure from the optical layout of conventional photometers has been made, based on previous experience with photometers on small telescopes. Reasons are given for the selection of various mechanical and electronic components and for their arrangement in this particular system. The finished instrument was employed to obtain 40 observations of the peculiar A-type variable star HD 124224 (CU VIR) during the 10 day period March 21-30, 1975 at Kitt Peak, Arizona. The light curves of this star in the natural uvby system of the photometer are presented and transformations to the standard uvby system are derived. The star appears essentially unchanged since first observed for light variations in 1955. In operation the photometer proved to be mechanically stable and convenient to use.

ACKNOWLEDGEMENTS

It is my pleasure to express my gratitude to the many persons who assisted me in the work of the project and the writing of this thesis. My supervisor Dr. D.P. Hube suggested the project, assisted in the design of the photometer and carefully read and corrected the manuscript. His generous provision of funds allowed me to travel to Toronto in 1974 and to Kitt Peak in 1975. Both trips provided invaluable experience in astronomy in general and photometry in particular. To the technicians who worked so hard in the production of the apparatus I am especially grateful. Mr. E.A. Foster did the mechanical work with his usual excellence, Wayne Sherrard persevered through my continually adding to the interface while it was under construction and John Woolley patiently performed hundreds of connections in the assembly of the electronics. During the observing session Dr. J. Winzer kindly introduced me to the techniques of differential photometry and the reduction of data. Finally I wish to thank my wife Kerrie for her patience during the late nights and her support throughout the entire project.

TABLE OF CONTENTS

LIST OF TABLES

LIST OF FIGURES

CHAPTER 1

INTRODUCTION

1.1 History of Photometry

The apparent brightness of a star is one of the most fundamental pieces of astronomical data. This quantity was first investigated by Hipparchus around the year 130 BC. He classified stars according to a scale of visual brightness which was to form the basis of the magnitude scale in use today. It was not until twenty centuries later that his naked eye estimates of star brightnesses were replaced by more accurate measures. In the last half of the nineteenth century, visual photometers were devised which worked on the principle of comparing the star in question to an artificial star. The brightness of this artificial star could be adjusted on a calibrated scale until the two stars appeared equally bright to the observer. The brightness of the unknown star could then be measured from the scale. The accuracy of this method was obviously limited by the vision of the operator, and the results obtained by different operators did not agree well. This was particularly true when the star to be measured was not the same colour as the artificial one.

Around the turn of the century, visual photometry was supplemented by photographic photometry. This was based on the relationship between the brightness of a star and the size and density of its image on a photographic plate. This method had the advantage that large numbers of stars could be recorded with one exposure for later analysis. This property made the photographic technique particularly useful in performing surveys of star magnitudes, and it was employed by Seares at Mt. Wilson between 1914 and 1922 to establish a list of 152 stars near the north celestial pole (the "North Polar Sequence") whose magnitudes were to serve as standards for the calibration of the magnitudes measured at other observatories. Such calibrations were necessary because the optical aberrations (astigmatism, coma, etc.) produced by each telescope influenced the measured photographic magnitudes, making the comparison of results from different telescopes rather difficult. There were other limitations imposed on the accuracy of the photographic technique. These resulted from the nonlinear response of the blackening of photographic material when exposed to extreme light levels, and the difficulties associated with maintaining exactly equivalent conditions during the exposure and processing of every plate.

During the same time period, attempts were being made to measure the brightness of stars by means of a photoelectric cell (Stebbins 1907). These had the advantage that the photocell current was linearly related to the flux of light over a wide range, making the process of data analysis much simpler than in the photographic method. However, the first devices used had such low sensitivity that their use was restricted to the brightest stars. The most important development in photoelectric cells for photometry was the introduction of a high gain current amplifier stage having the form of a series of electron emissive surfaces. This "electron multiplier" was housed in the same evacuated glass envelope as the photoemissive cell and the entire device was called a "photomultiplier tube". Around 1950 a very successful form of such a tube was produced by RCA having the model number 1P21. This tube had such high sensitivity and low noise that it quickly became a standard component of astronomical photometers. Johnson and Morgan (1953) used this tube when defining the first standard three colour photometric system (the UBV system) and it has remained in widespread use since that time. In modern photometers this tube is sometimes replaced by newer devices having more ideal characteristics (higher sensitivity or lower noise), and the standard three colour filter set of

Johnson and Morgan is often replaced by, or used in conjunction with, other filter sets designed for special purposes.

1.2 Photoelectric Photometers

The principles of operation of a photoelectric photometer are quite simple. An image of the star in question is formed by the telescope objective on the surface of an opaque plate which is pierced by a small hole, called the diaphragm. This opening permits only the light of the desired star to reach the photomultiplier, eliminating the light from any nearby stars, and most of the background light of the sky itself. Since the emissivity of the photocathode may vary with position across its surface, it is necessary to ensure that motion of the star image within the diaphragm does not cause the starlight to strike different parts of the cathode as this would produce apparent changes in the intensity which are not real. This is prevented by means of a lens, first employed by M. Ch. Fabry of the Paris Academy of Science in 1934. The Fabry lens is used to form an image of the telescope objective on the photocathode surface. This image fills most of the available cathode area to prevent saturation effects and is virtually fixed in position for any location of

the star image within the diaphragm. In this way the measured intensity is made independent of any wander of the star image due to faulty tracking of the telescope.

The location of the star of interest requires that viewing eyepieces be introduced into the optical path, a wide angle one in front of the diaphragm for coarse positioning of the star and a high magnification one after it for exact centering of the image in the diaphragm. In addition, it must be possible to place filters between the Fabry lens and cathode and to select any one of several sizes of diaphragm hole. The ways in which these requirements have been met in the design of this photometer are outlined in the following chapter.

1.3 Signal Handling in Photometry

In concluding this introduction, a brief description of recent changes in the signal handling techniques used in astronomical photometry is in order. When photomultiplier tubes were first introduced, the signal current was treated in an analogue fashion. This means that the current pulses produced by photon impacts on the cathode were integrated over time without any selection process being applied. Usually the output

current pulses were passed through a large resistor and the resultant fluctuating voltage appearing across this resistor was fed to an integrating amplifier. The resulting output voltage was recorded by means of a printing digital voltmeter, chart recorder, or similar device. One disadvantage of this technique is that photomultipliers produce spurious output pulses (noise) due to thermal emission of electrons from the stages in the electron multiplier (the dynodes). The analogue technique has no means of separating these noise pulses from those pulses originating from photons striking the cathode. In addition, treating the intensity signal as an analogue voltage makes the output critically dependent on factors such as the resistance of the signal resistor and the gain of the integrating amplifier. Since these quantities can change with the age of the electronic components involved and the ambient temperature, an analogue photometry system has poor long term stability of output.

An alternative signal handling technique which is becoming increasingly popular is the digital photon counting process. In this technique, a high gain, wide bandwidth current amplifier is used to amplify directly the individual current pulses produced by the photomultiplier. These are then sorted according to

amplitude, and only the largest ones are fed to a high speed electronic counter. Since the amount of current in each pulse depends on the number of dynodes it has traversed in the photomultiplier, this discrimination process can be used to select pulses originating at the cathode out of a collection of pulses of both cathode and dynode origin, since pulses of cathode origin have the largest amplitude. The discrimination process gives digital photon counting a superior signal to noise ratio to that of analogue photometry. In addition, the digital process has superior long term stability since the number of pulses counted is independent (in first order) of the amplifier gain, so any change in the gain due to age or temperature effects will not directly change the measured intensity of the starlight.

It should be noted that to produce a pulse large enough to be counted with low impedance electronics (which should be used to maintain high immunity to induced noise), the overall multiplication of each photoelectron must be by a factor of the order of 10^9. There are photomultipliers available today with gains as large as this, but in general they have relatively poor long term stability when operated at maximum gain. In order to maintain maximum reproducibility of the results, the gain should not exceed about 10^6. This means that

further amplification by a factor of 10^3 must be supplied by the photon counting electronics.

The use of a broadband amplifier with this high gain value requires that careful shielding of the inputs be used to prevent the system from responding to induced signals, particularly in the radio frequency region.

Because the amplifier and discriminator electronics have finite bandwidth, and because the photomultiplier output pulses have finite width, a photon counting system will give incorrect measurements if excessively high count rates are used. This happens because the system cannot respond to a second pulse for a finite time (called the "deadtime") after the arrival of an initial pulse. It was this factor that delayed the use of the photon counting technique in astronomy until recent years, since only modern solid state amplifiers retain enough bandwidth at high gains to give acceptably small system deadtimes. For a counting system with deadtime d, the true count rate N can be approximated (Evans 1955) by $N = n(1 + nd)$ where n is the observed count rate. A good photon counting system has a deadtime of 30 nsec or less, meaning that the required correction is less than one percent for count rates less than 3×10^5 counts/sec. If observations of bright stars produce count rates higher than this, the overall

system gain should be reduced to lower the count rate to an acceptable figure, as the application of the necessary correction to each count is a tedious process.

The photometer designed and built in this project utilizes photon counting data acquisition. The selection of the appropriate electronic components for the system is discussed in Chapter 3, and in Chapter 4 the results of an observing program using photon counting photometry are presented.

CHAPTER 2

THE MECHANICAL DESIGN

2.1 Design Criteria

From the general description of the functions of a photometer given in Chapter 1, it should be apparent that a variety of mechanical arrangements are possible in the construction of a photometer. In practice, the design of a photometer for a particular telescope involves a larger number of constraints than are predicted by the general theory of operation. The purpose of this chapter is to show how the final design of this photometer arose out of the additional requirements imposed in this case.

One of the most important considerations for any auxiliary device to be mounted onto a small telescope is the total mass. Whenever an instrument is attached to a telescope, additional weights must be added to restore the balance of the telescope around both the declination and right ascension axes. Limits are imposed on the total mass that any instrument and its counterweights may have by the strength of the telescope mounting and the ability of the electric motor drives on the axes to operate under the increased moment of inertia.

However, while maintaining the lowest possible mass, the photometer must be mechanically stable enough to ensure very solid mounting of the optical components. The centers of the diaphragm, Fabry lens and photocathode should not deviate from the optical axis by more than 0.005 inch, and the latter two must be mounted perpendicularly to the axis as accurately as possible. These precise alignments must be maintained with the instrument in any attitude it may assume when the telescope is pointed to various parts of the sky. To achieve the best compromise between strength and mass, virtually all of the parts of the photometer made locally are of duraluminum metal.

2.2 Optical Design

In addition to being internally stable, a photometer must also be very securely attached to the telescope. To ensure this stability our photometer incorporates a somewhat unorthodox optical path. Normally, photometers are arranged parallel to the telescope optical axis (see fig. 2.1). However, this type of photometer has been used at this University in the past (Brown 1968) and we have found that the large distance of the center of mass from the small area of contact with the telescope makes this photometer

susceptible to flexure. This flexure causes the diaphragm to move with respect to the optical axis (Tomaszewski 1974), changing the critical alignment of the optical components. To avoid this problem, we have included a mirror at a 45° angle to make the optical axis of the photometer perpendicular to that of the telescope (see fig. 2.2). This keeps the centre of mass of the photometer close to the telescope and increases the area of contact for mounting purposes. To centre the mass of the photometer about the telescope axis as much as possible, this mirror is made to rotate through 180° around the axis. This allows the field viewing eyepiece to be located on the opposite side of the axis from the diaphragm and photomultiplier (see fig. 2.3), and also allows this rotating mirror to perform the dual functions of bending the optical path and allowing the field viewing eyepiece to be inserted into the optical path for coarse positioning of the star image.

The insertion of the diaphragm viewer into the optical path is accomplished by a conventional sliding mirror arrangement (fig. 2.4). The control for this mirror is designed to perform other functions associated with the diaphragm viewing sequence at the same time. In order to centre the star image in the diaphragm it

Fig 2-1 Linear Photometer Fig 2-2 Folded Photometer

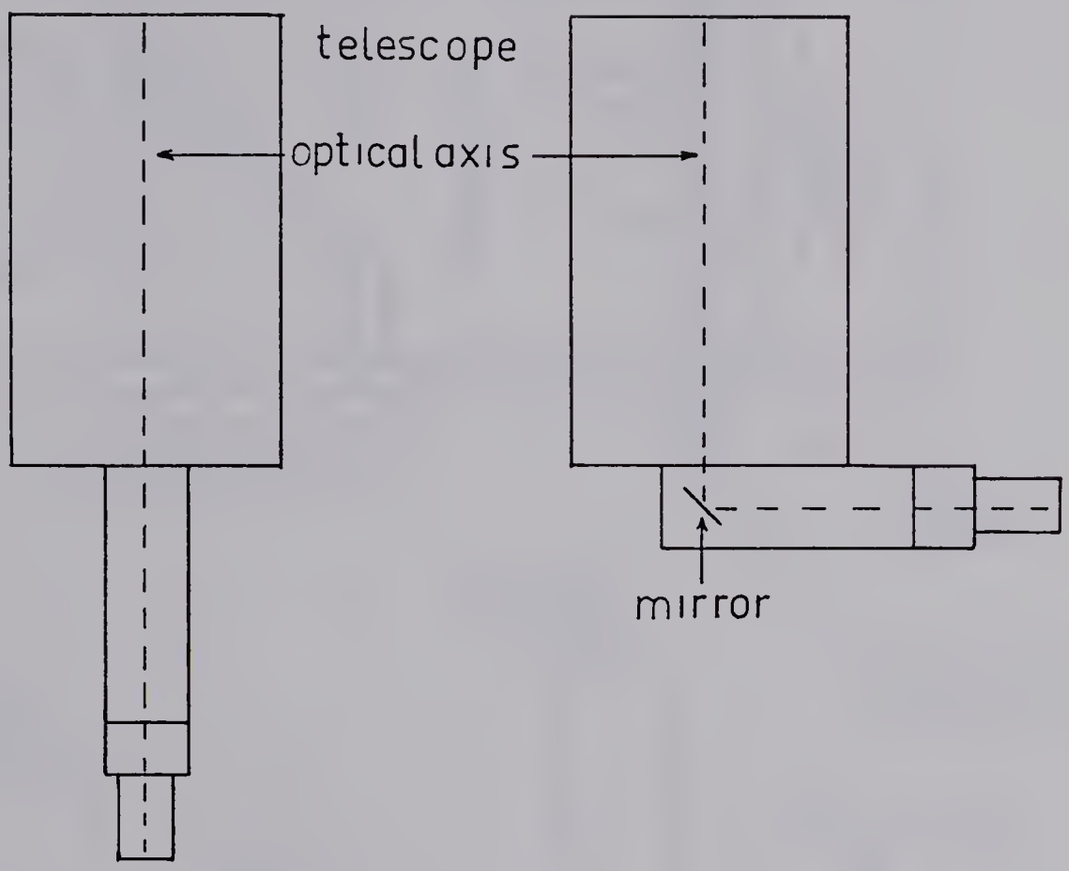

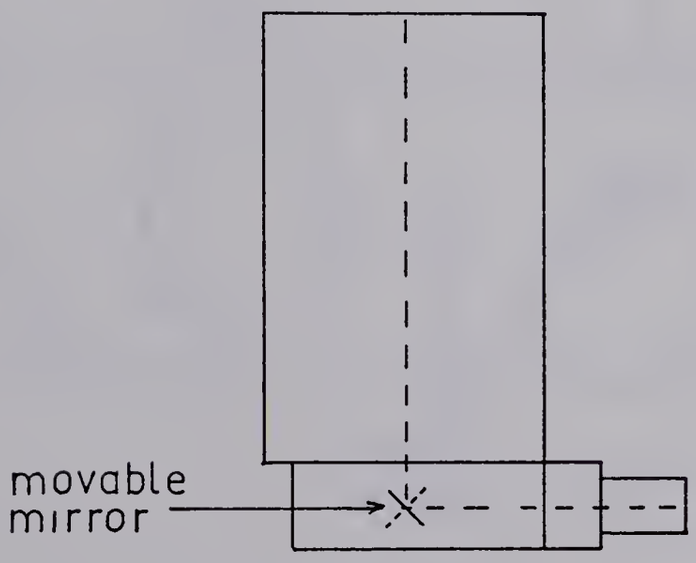

Fig 2-3 Folded, Centred Photometer

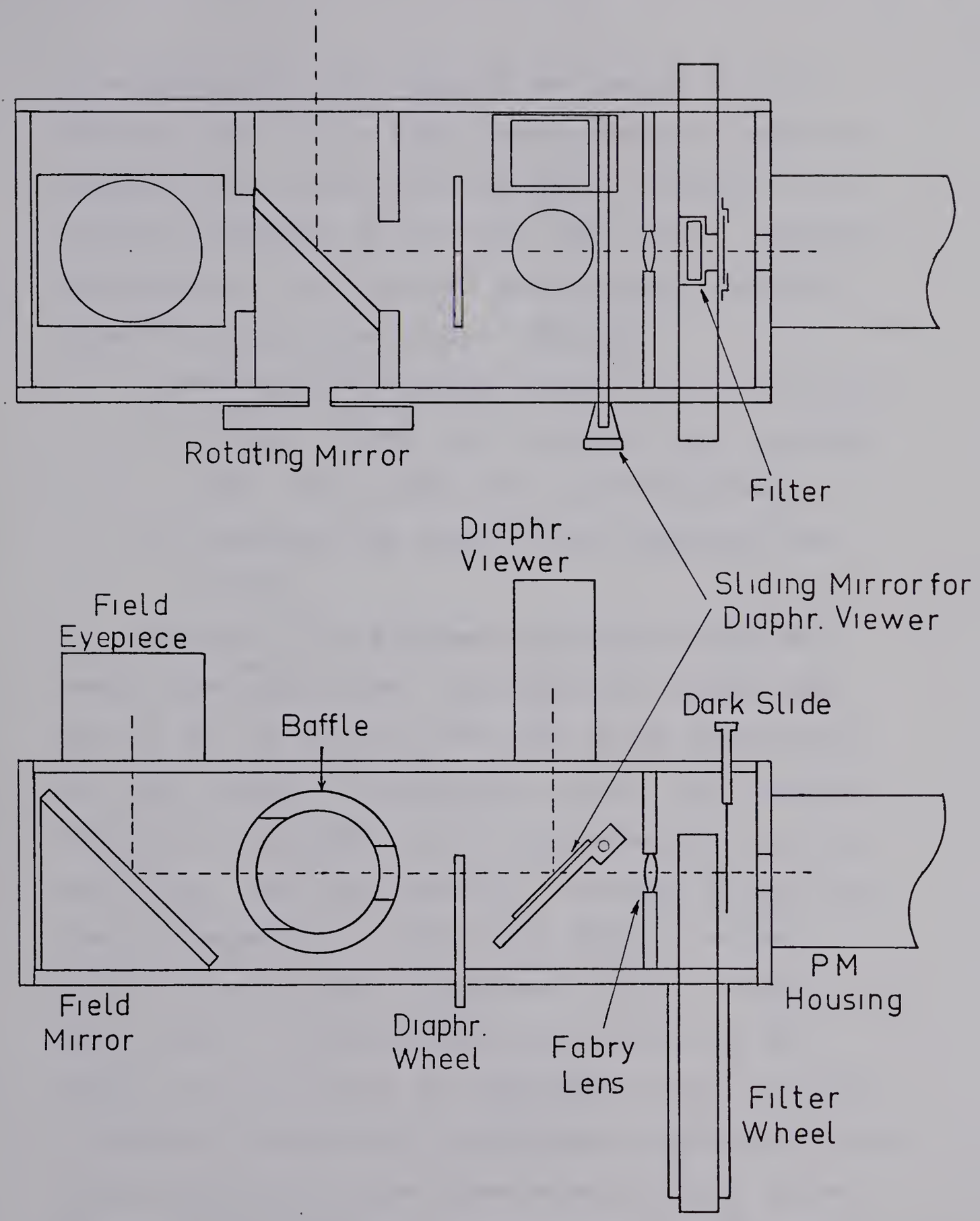

Fig 2-4 The Photometer

is necessary that the edges of the opening be illuminated, and before a light can be turned on near the diaphragm, the photomultiplier must be shielded or it could be overloaded by the high light level. Operating the diaphragm viewer control is thus made to perform three functions sequentially. They are:

1) Moving the diaphragm viewing mirror into place.
2) Sliding a cover over the Fabry lens to prevent light from reaching the photomultiplier.
3) Connecting the power to the diaphragm illuminator.

Because of the extremely high sensitivity of modern photomultipliers, the possibility exists that some of the red ambient light used in the observatory for chart reading could register on the tube output by entering the eyepieces of the photometer when they are not in use. This is prevented in the case of the field viewing eyepiece by a baffle tube which is sealed against entering light by the back of the rotating mirror when it is reflecting light towards the diaphragm. In the case of the diaphragm viewing eyepiece, a shield is included on the diaphragm viewer shaft which covers the inside of the viewer when it is not in use. These two provisions seal the photometer against the entry of ambient light.

2.3 The Illumination System

Since it is to be operated in semi-darkness, four lamps are included in the photometer to help the observer use the controls. Two of these illuminate the cross-hair of the field viewing eyepiece, one shines on the diaphragm and one on the filter identification letters stamped on the outside of the filter wheel. In each case, a light emitting diode (LED) was chosen over a conventional light bulb because of longer service lifetime, small size, and deep red colour. All of these lights are actuated by one microswitch in the diaphragm viewing assembly, so none can be turned on without the photomultiplier shielding slide being in place over the Fabry lens. Power for the LED's enters the photometer through a BNC connector at the field eyepiece end, and the light level can be adjusted with a knob located adjacent to this connector. The lamps require +12 volts DC. This voltage must not be exceeded and the correct polarity must be supplied or the diodes will not give light. The circuit diagram for the illumination system is shown in fig. 2.5.

2.4 The Filter System

The photometer has been designed with a capacity of six standard one inch square photometer filters.

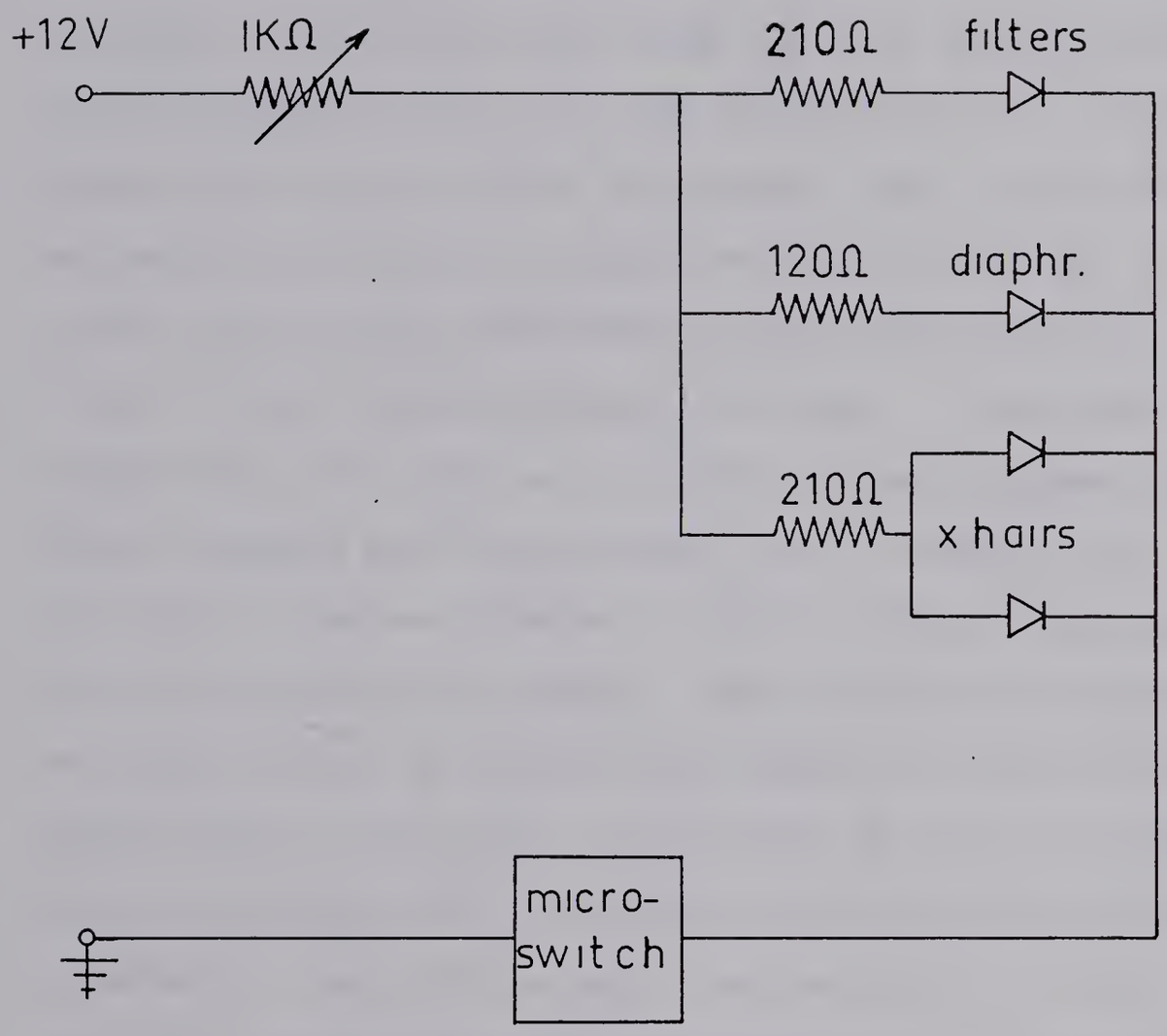

3 LEDs are std. HP type, diaphr. LED is Fairchild model FLV-104 (narrow beam)

Fig 2-5 Illumination System Circuit Diagram

The filter system was designed as a wheel rather than a linear slide in order that it be kept as compact as possible. The first wheel made has been stamped with identification letters for the four colour uvby filter system and the two filter H_β system. The filters are selected by rotating the wheel to the one of six preset click stops which brings the identification letter of the desired filter into view. Additional wheels are to be made up for other filter systems for which frequent need is foreseen, and to change the photometer from one system to another these wheels can be interchanged quite easily. Special mention should be made here of the precautions taken to prevent filter damage due to the cold. In the past we have had interference filters suffer delamination of the glass layers, presumably caused by pressure exerted on their edges when the duraluminum holder contracted at low temperatures. To prevent this unfortunate (and costly) problem from recurring, the filter wheels use pieces of plastic foam as spacers to allow for differential contraction of the glass and metal without applying pressure to the filters. The arrangement of spacers is shown in fig. 2.6.

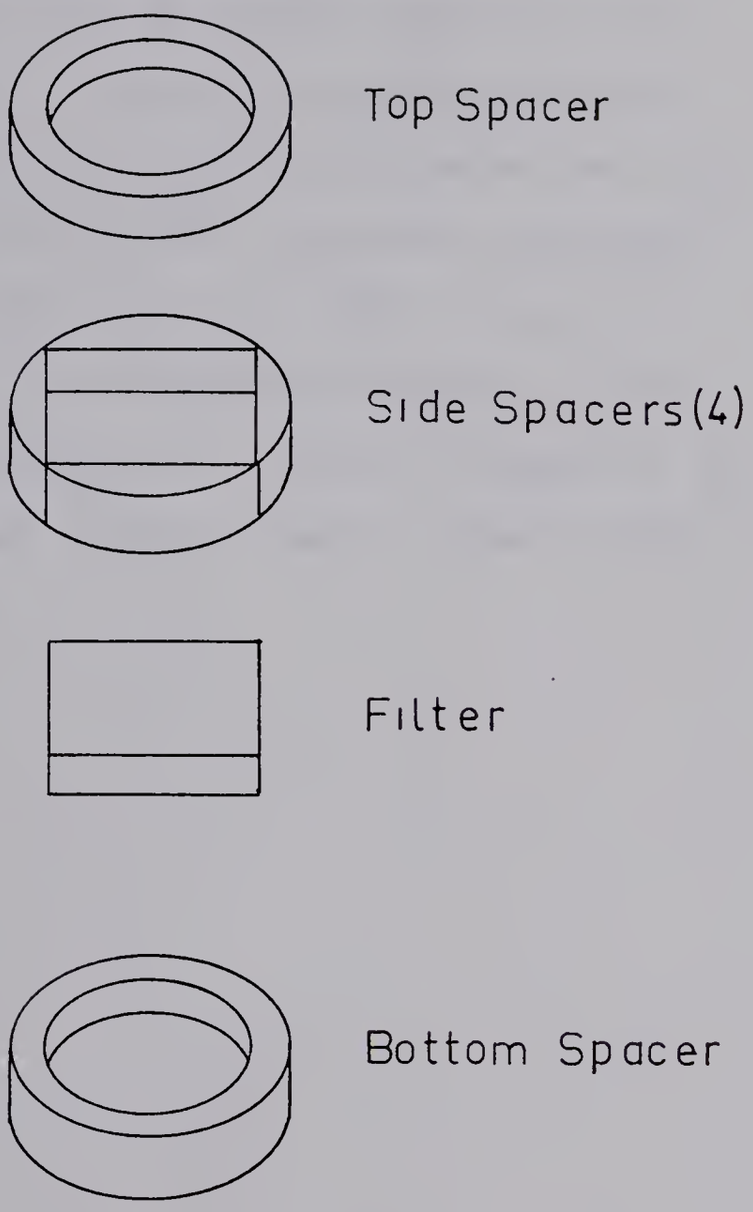

Fig 2-6 Plastic Foam Spacers in Filter System

2.5 The Diaphragms

The diaphragm wheel has been drilled with five openings whose sizes were chosen to give angular diameters of 5, 10, 20, 30 and 40 seconds of arc when the photometer is used at the f/18 focus of the 20 inch telescope. These are selected by rotating the wheel to one of five click-stop positions. At each of these positions the angular size (in seconds of arc) of the diaphragm in place in the optical path is displayed as a number stamped on the portion of the wheel that is visible outside the wall of the photometer.

CHAPTER 3

THE ELECTRONIC DESIGN

3.1 Choice of Components

In addition to the design and construction of the mechanical and optical parts of the photometer, the project involved the assembly of existing and newly acquired electronic equipment into a digital photon counting system. The new equipment purchased for this project was made by Ortec Inc. and includes the following devices:

Model 9301 preamplifier

Model 451 spectroscopy amplifier

Model 436 discriminator

Model 772 counter

Model 719 timer

These devices are mounted in a model 401A modular system rack with internal power supply (see fig. 3.1). The Ortec equipment was chosen over other brands for two main reasons. First, it has a large range of selectable values of the operation parameters. The total gain may be varied from 25 to 30,000, the discriminator threshold voltage from 50 to 500 mv and the count interval duration from 0.1 to 8000 seconds. This selection allows the system to be adapted to a wide

Fig 3-1 The Ortec Rack Containing the Ortec Modules and the Printer Interface

variety of observing programs and observing conditions. The method of selecting an operating point for the system from this range of parameters is discussed in Chapter 5.

The second important feature of the Ortec equipment is its modular design. The present rack has room for several additional modules, so the system can be expanded in the future at minimum expense. For example, by duplicating the amplifier and counter modules this equipment could be used with a two channel photometer. Another advantage of the modular design is that if repairs become necessary only the faulty module need be returned to the factory, and chances are that a replacement could be borrowed from one of the many Ortec systems in use in the Physics Department if the need was urgent.

3.2 Choice of the Photomultiplier

The photomultiplier used is an EMI 9502S which has been selected from a batch of these tubes especially for use in a photon counting system. This tube is well suited to the Ortec electronics and has been used by the Astrophysics group for several years (in 6256 form, having quartz window) with very satisfactory results. This tube is of somewhat more modern design than the

RCA 1P21 and has the advantages of higher gain and sensitivity while producing less noise than the standard tube. Table 3.1 shows the gain and dark current values for a typical tube of each type when operated at the recommended voltage, and fig. 3.2 shows the spectral response of the two cathodes (on separately normalized scales).

Table 3.1
Photomultiplier Specifications

	RCA 1P21 (at 1 kv)	EMI 9502S (at 1.7 kv)
Gain	2×10^{6}	1×10^{8}
Sensitivity	200 amps/lumen	5000 amps/lumen
Dark current equivalent input	5×10^{-10} lumen	3.5×10^{-14} lumen

Since the cathode response curves are not identical, transformations are needed to convert the results obtained with the 9502S to those of standard magnitude systems. A program of observations of standard stars was done along with the variable star work to allow the calculation of the required transformations. These are presented in Chapter 4.

3.3 The Electronic Interface

The major task of the development of the electronics was to adapt the Hewlett-Packard (model 562A)

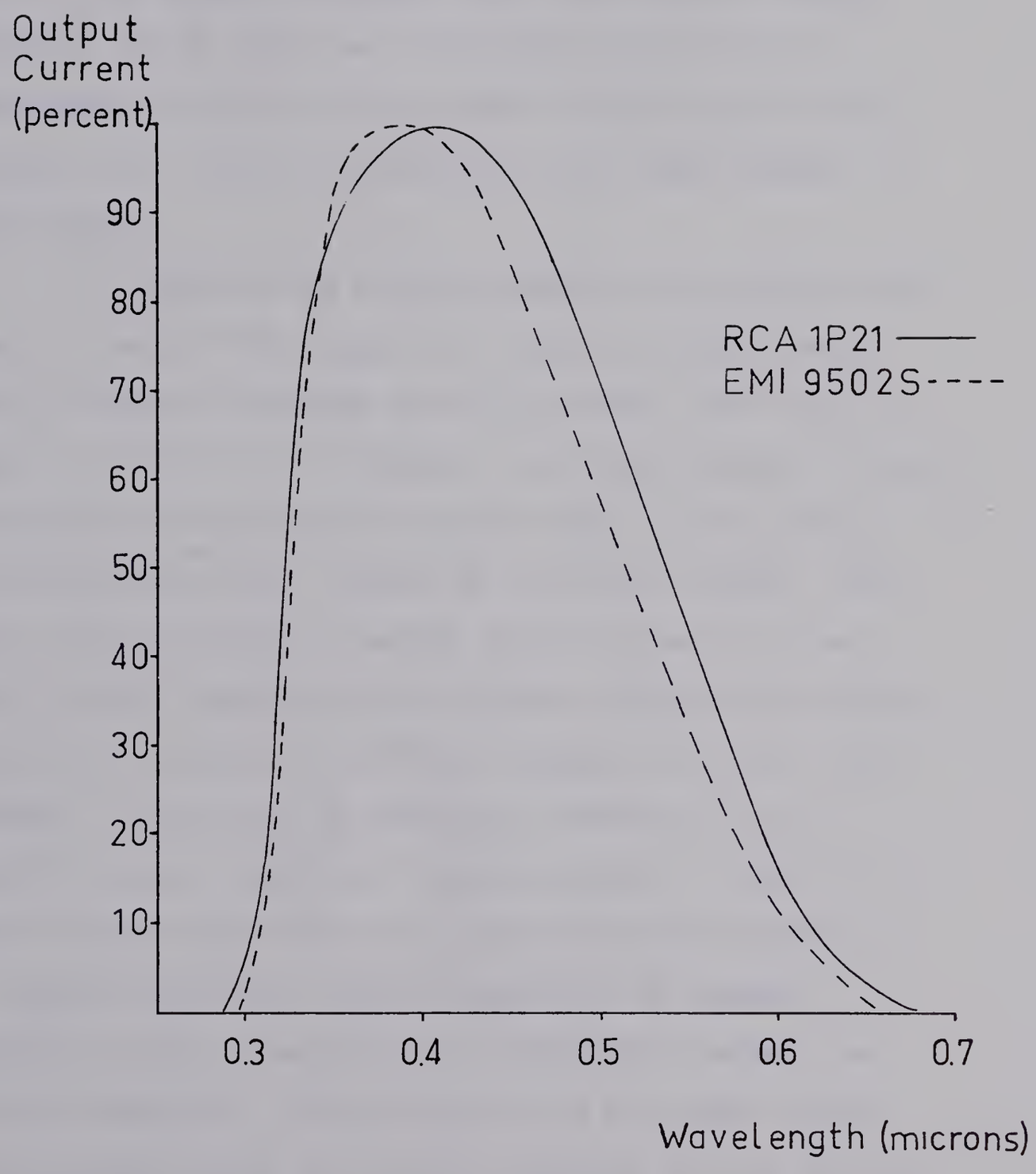

Fig 3-2 Cathode Response Curves

eleven column line printer, which was used as part of the previous analogue photometry system, to the printing of the results obtained with the photon counting system. To do this, an electronic interface was designed and built into an Ortec module chassis which mounts into the rack occupied by the Ortec modules of the system.

In the previous analogue system, the printer was used to record the output of a Hewlett-Packard model 3440A digital voltmeter in five columns, and that of a digital clock in six columns. For this purpose, it was equipped with six input circuit cards for the binary coded decimal (BCD) output of the clock (format +1248 BCD) and six cards, of which only five were in use, for the BCD output of the voltmeter (format +1224 BCD). Since the output of the Ortec counter is in the +1248 format it could not be directly connected to the printer as the voltmeter output had been. Since five more +1248 format cards were prohibitively expensive, a format conversion circuit was built to change 5 digits of data from +1248 to +1224 BCD to permit use of the old cards. This circuit and its power supply are mounted inside the printer chassis and are used to print the time data in the first five columns of the paper. The tens of hours digit has been omitted, due to lack of column capacity. The output of the Ortec

counter goes directly into the +1248 cards and is printed in columns 6 through 11.

The main purpose of the printer interface is a data format conversion made necessary because the Ortec counter is designed to print through an Ortec modified teletype, one character at a time, while the Hewlett-Packard printer prints eleven characters simultaneously. The interface performs this conversion by first taking the place of an Ortec 432A print controller in preparing the counter to present its data. The waveforms necessary to do this are called "print command" and "start data transfer" in the Ortec counter manual (p.7). It then causes the six characters to appear in turn (in BCD form) at the four data outputs of the counter by generating six clock pulses (called "print advance" pulses in the Ortec counter manual). The interface contains a data buffer consisting of six sets of four binary latch registers which are connected in parallel with the four data outputs of the counter. These are enabled in turn by a binary shift register which is advanced by the "print advance" clock pulses (see block diagram fig. 3.3).

When the sixth character has been stored, the interface commands the printer to print the stored data and the current time. It then resets the counter,

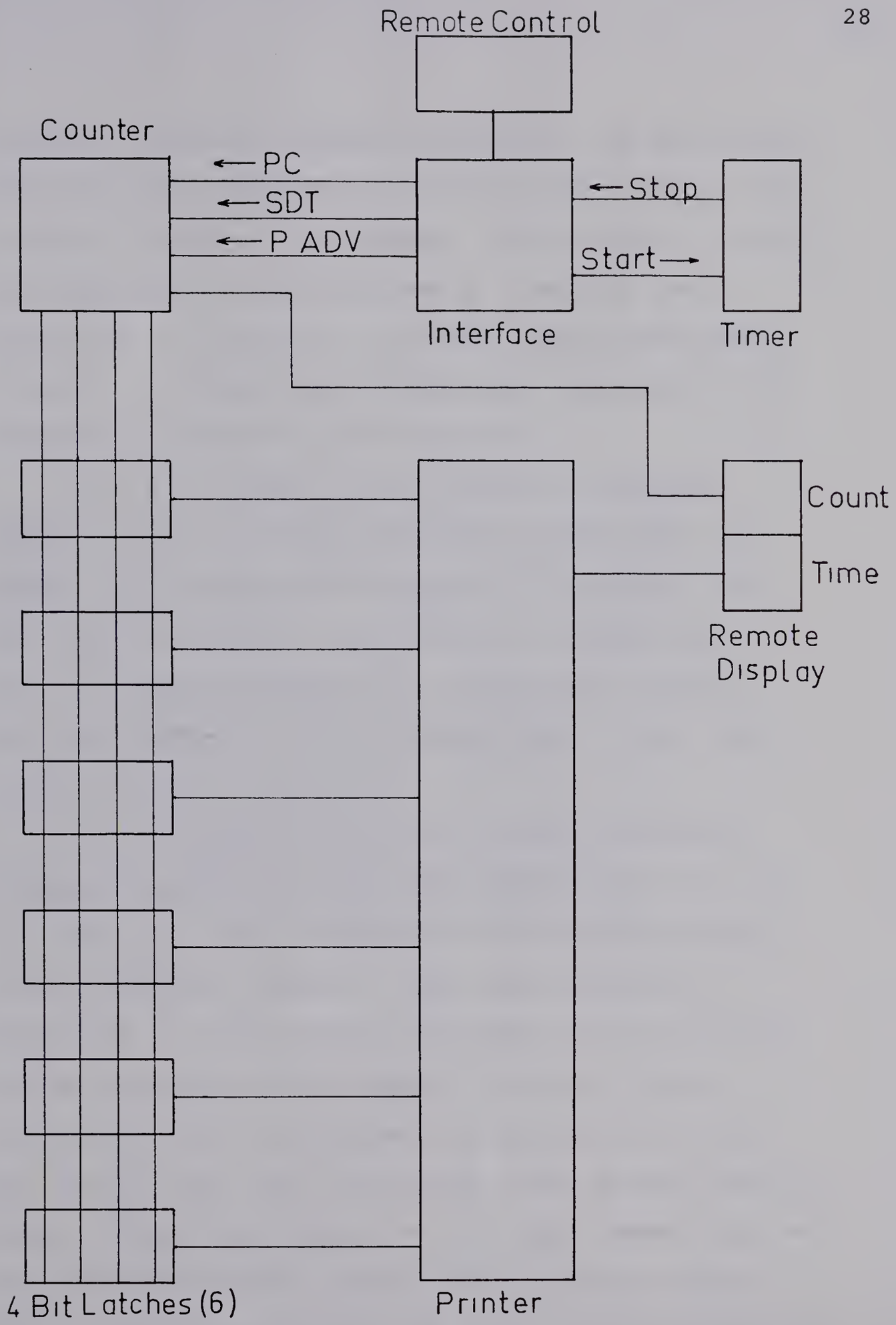

Fig 3-3 Electronic Block Diagram

latches, and shift register, and awaits the next signal from the Ortec timer that a count interval is over and a count is ready to be printed. "Print advance" pulses are generated in the interface at a rate of one Kilohertz, so the entire interface cycle takes about 10 msec. An additional 160 msec are required for the mechanical operation of the printer.

The final phase of the electronic interface project is the provision of remote control over the photon counter and remote display of the data. This was made necessary by the decision to locate the photon counting equipment and printer in a heated building adjacent to the telescope dome, rather than in the unheated dome itself.

The observer in the dome controls the photon counter by means of a hand held control box (fig. 3.4). This box contains an extension of the timer's "start" button (labelled "count"). When this button is depressed, a count interval of preset duration begins and an extension of the timer's "interval" light (labelled "count in progress") is provided to inform the observer how long the machine stays in the counting mode. While this light is on, no other commands may be issued to the photon counter from the remote control box. A second light below the "count" button (labelled "overflow") is activated whenever more than 999,999

Fig 3-4 The Remote Control Box

events are counted in the preset interval of time. Once this light comes on, it can only be extinguished by pushing the button labelled "error", which clears the overflow condition and prints negative signs in the data columns (6-11) to indicate that the previously recorded count is invalid because of counter overflow. The "error" button may also be used by the observer to indicate that the previously recorded count was performed on an imperfectly aligned star image, through the wrong filter, or is to be ignored for any other reason. It should be noted that the print follows immediately after the "error" button is pushed; there is no counting interval delay.

The final pushbutton (labelled "filter") is used in conjunction with the digital rotary switch below it to make coded notations on the printed output. Pressing the "filter" button causes an immediate print of negative signs in columns 6 through 10 and of the number shown on the rotary switch in column 11. By making up his own coding system, the observer can use this switch to indicate which objects are represented by the various counts appearing on the printed results (variable star comparison star, sky) and which filter was used, without the keeping of handwritten notes.

These three pushbuttons and both operating lights are duplicated on the front panel of the

printer interface to permit operational checks to be carried out without numerous trips back and forth between buildings. They also provide the observer with completely remote control observing (in one colour), the duration of which is limited only by the tracking accuracy of the telescope drive.

The count total is displayed on the front of the Ortec counter, and the digital time is shown on the clock mounted inside the printer. In addition, both of these are displayed on a slave digital readout mounted inside the observatory dome (see fig. 3.5). This information is provided to allow the observer to monitor the results being recorded and check on the quality of the sky conditions. The last photon count is retained on the display until replaced by the next one, a feature which allows the observer to see quickly how repeatable the results are by watching how many of the six columns change when the count is updated.

The time is displayed in six digits, tens and units of hours, minutes and seconds. The time base of the clock is the frequency of the power line, which will maintain an accuracy of one or two seconds over the longest possible observing session. Although this frequency is adjusted to maintain electric clocks with sufficient accuracy for household purposes, the error on any given night may be as much as a minute or more.

Fig 3-5 The Remote Digital Display

For this reason the clock should be set to a radio time signal (CHU or WWV) at the start of each night of observing.

CHAPTER 4

THE OBSERVATIONS

4.1 The Test Observing Program

The photometer designed in this project will be used on the 20-inch telescope now under construction to replace the existing 12-inch instrument located at the University of Alberta Observatory near Devon, Alberta. However, since this telescope will not be in operation before 1976, another telescope of suitable size and focal ratio had to be found for use in the initial testing of the photometer.

Observing time was available on a 16-inch telescope at the American National Observatory facility at Kitt Peak, Arizona, and the photometer was quite easily adaptable to being mounted on this telescope, so it was chosen for the testing. A program of observations of the peculiar A type variable HD 124224 (CU VIR) was carried out between March 21 and 30, 1975, for this purpose.

4.2 A_p Variable Stars

The stars designated as class A_p were first recognized during the compiling of the Henry Draper Catalogue of stellar spectra between 1911 and 1915 by

the astronomers of the Harvard College Observatory. It was discovered that a number of stars showed spectra similar to stars of the late B and early A classes, with the exception that they displayed abnormally strong lines of certain elements, commonly Hg, Mn, Si, Sr, Cr or one of the rare earths. These stars were put into the class A_p, the subscript meaning that the spectra were "peculiar". In subsequent years, observations of these stars have shown that they have a number of unusual physical characteristics.

The unusually strong spectral lines that first drew attention to the stars are indicative of abnormal chemical composition. The elements producing the peculiar lines in a particular star may be more abundant than would be expected in a normal star of the same spectral class by a factor of 100, or more. Furthermore, Deutsch (1947) showed that the peculiar lines in the spectra of some A_p stars showed periodic variations in strength and later (Deutsch 1956) he showed that the period of these spectral variations was correlated with the widths of the lines, an indication that the apparent changes in chemical composition causing the line strengths to vary are related in some way to the rotation of the star. During this same time period Babcock (1947, 1958) had discovered that the spectral lines of A_p stars showed Zeeman splittings

indicative of large magnetic fields, ranging in strength from a few hundred to several thousand gauss. He also observed that in some stars these fields were periodically variable.

A final puzzling aspect of the peculiar A star story was the discovery that most magnetic A_p stars showed overall variations in their light output. These were found to be typically a few hundredths of a magnitude in amplitude and to have the same period as the spectral variations.

Numerous hypotheses have been advanced to explain the observed behavior of the A_p stars. Some authors supported surface nuclear reactions or magnetic accretion of material from space as explanations for the abnormal compositions. The hypothesis which seems best able to account for the observed phenomena is the oblique rotator model. In this model, the star has a strong dipole magnetic field (as large as several kilogauss) whose axis is inclined to the axis of rotation. This strong field serves to stabilize the star's atmosphere against convection, giving sufficient stability for the diffusion of various heavy elements outward from the interior. The elements which appear at the surface are those having the largest cross-sections for photon collisions. These are more strongly affected by radiation pressure than by gravity (Michaud

1970). The zones of abnormal composition are thus associated with regions of maximum atmospheric stability, and these are probably near the magnetic poles. These factors combine to present to the observer a star whose apparent composition and magnetic field strength vary with the rotational period.

The observed variability in light is explained in this model by the higher atmospheric opacity characteristic of the regions of abnormal composition. Radiative flux trapped by these zones of abnormally high opacity is reradiated at some other wavelength, since the absorbing material is heated in the process. When the star is observed in a limited range of wavelengths (as through a photometric filter) these patches of abnormal abundance can appear either darker or brighter than the normal parts of the star's surface, depending upon whether the wavelength band used is a region of abnormal absorption or abnormally high emission due to reradiation. In either case the star's brightness will appear to change as the patches rotate across its visible face.

4.3 The Star HD 124224

The A_p star HD 124224 was first observed to be a spectrum variable with an abnormally high abundance of

silicon by Deutsch (1952), and later Hardie (1958) showed that the star varied in light with the same period as the spectral variations.

This star is well suited to a brief test observing program, since it has a very short period (about 13 hours) and shows relatively large amplitude light variations ($0.^{m}14$ in U). These two properties are both desirable if a good light curve is to be obtained in a few nights of observation. In addition to photometry in the uvby system, the observations included photometry with interference filters designed to measure the equivalent widths of Si II spectral lines. From the oblique rotator model we would expect the silicon lines to show maximum strength at maximum light, since the variability of the star according to this theory is due to the opacity of Si II in the far ultraviolet causing increased flux in the near ultraviolet and visible regions of the spectrum. The filters used were designed to provide an effective measurement of the equivalent widths of the lines at 4128 and 4131 Å by comparing the flux received through a narrow filter (FWHM 10 Å) centered on 4130 Å to that of a wider filter used to measure the flux from the nearby continuum. The center of the wide filter (FWHM 100 Å) was displaced towards the red to 4180 Å to prevent the wings of the Hδ line at 4101 Å from interfering in the silicon measurements.

4.4 Observational Techniques

The Kitt Peak #4 16 inch telescope is a Boller and Chivens instrument with a Cassegrain focal ratio of f/18. It is equipped with two separate data acquisition systems for photometry. The analogue system uses a charge integration circuit with output via chart recorder or voltmeter, and the photon counting system uses an SSR Instruments Co. model 1120 amplifier-discriminator and a model 1108 timer and counter.

It had been intended that the photon counter be used throughout the experiment, but problems were encountered on the first night of observing with large noise counts of unknown origin, and the analogue system was used on that night. During the next day, the large noise counts were traced to noise from the high voltage supply being induced into an improperly shielded signal cable. When the shielding problem was corrected and a filter introduced into the high voltage line the problem was corrected. The photon counter was used for the remainder of the observing session. A circuit diagram for the high voltage filter used is shown in Chapter 5.

4.5 Observing Procedure

The technique of observation used was to take

five ten second counts through each filter (uvby, Si wide, Si narrow) on the comparison star HD 122408 (τVIR) and then offset the telescope slightly and take one ten second count through each filter on the sky nearby. This was followed by a similar set of counts on the variable star (CU VIR) and its neighbouring sky. Throughout the observing session a diaphragm size of 25 arc seconds was used at all times. This cycle of observations was repeated as quickly as possible throughout the hours when the stars were high enough in the sky that the differential air mass between them was less than 0.05. This ensured that the magnitude correction for extinction effects would be correct to within ± 0.005.

These observations were interrupted nightly for the observation of standard stars having known magnitudes in the uvby system. This work was necessary to allow the transformation of the derived magnitudes to magnitudes in the standard uvby system of Stromgren (1963). In section 4.10 below a list of the standard stars is given and the transformation equations are listed along with a table of the coefficients resulting from a linear least squares fit of these equations to the data.

4.6 Data Reductions

The reduction of the raw count data into magnitudes was done by averaging each set of five counts, subtracting the sky count taken through the same filter, and finding the resulting number in a table of values of the function $m = -2.5 \log (\text{count}) + 15$. The resulting magnitudes were shifted away from the standard magnitudes of each star by constants which depend on the overall sensitivity of the photometric system. However, in differential photometry the difference in magnitude between the variable star and the comparison star (which is chosen to be of constant brightness) is independent of this constant.

4.7 Extinction Corrections

The differential magnitudes which result from this process must next be corrected for the effects of the passage of the light through the Earth's atmosphere. This is done by subtracting from the measured magnitude of each star a term consisting of a coefficient times the air mass through which it was observed. Subtracting this term from its magnitude assigns to the star the numerically lower magnitude which indicates the increased apparent brightness it would have when observed from outside the atmosphere. For the uvby magnitudes the

correction equations have the form:

$$u_c = u_{obs} - K_u X \qquad b_c = b_{obs} - K_b X$$

$$v_c = v_{obs} - K_v X \qquad y_c = y_{obs} - K_y X$$

where the subscript c denotes corrected magnitudes and the subscript obs denotes observed ones. The air mass X (Hardie 1962) is a function of the zenith angle of the star. A value of the air mass is calculated for each time of observation of each star observed.

Each extinction coefficient K is equal to the slope of the graph of the observed magnitudes of a standard star against the air mass at each time of observation. A separate graph is drawn for each of the four colours and the four slopes give the coefficient K_u, K_v, K_b and K_y. The comparison star τ VIR was used to measure these coefficients in this case and the resulting values are shown in Table 4.1.

Table 4.1

Extinction Coefficients

Date (March 75)	21/22	23/24	24/25	28/29	29/30	Avg.	Kitt Peak (Crawford)
Coefficients							
K_u	.67	.58	.50	.67	.72	.63	.646
K_v	.28	.40	.28	.37	.46	.36	.339
K_b	.27	.30	.18	.25	.27	.25	.218
K_y	.19	.20	.13	.20	.22	.19	.150

The last column shows the long term average values for Kitt Peak derived by Crawford and Barnes (1970). When comparing these results it should be noted that most observations have a differential air mass of 0.01 or less, so a change in the coefficients as large as 0.1 changes the calculated result by only 0.001 magnitude. This means that the changes in the coefficients caused by night to night variations of the sky conditions do not significantly affect the accuracy of the results. The table of coefficients gives an approximate measure of the atmospheric transparency on the five nights of observation. It shows that only March 24-25 had transparency better than average, as shown by extinction coefficients smaller than Crawford's average values for Kitt Peak.

No extinction corrections were calculated for the silicon photometry. The time between observations through the wide and narrow filters was usually less than one minute, a short enough interval to permit the assumption that the air mass was the same for both observations. The silicon index ΔSi ($Si_{narrow} - Si_{wide}$) calculated for each star is thus independent of atmospheric extinction and the differential index $\delta Si = \Delta Si(Cu) - \Delta Si(\tau)$ is therefore also independent of extinction effects, and no correction is required.

4.8 The Light Curves

In order that the results of observations made on successive nights could be compared, each time of observation in Julian days (JD) was converted to a phase of the cycle of light variation. This was done using the ephemeris published by Deutsch (1952) for the maximum strength of the lines of He I:

$$\text{He } I_{max} = \text{JD } 2434144.05 + 0.52067 \text{ day} .$$

The results of five nights of observation are shown in Table 4.2. The tabulated magnitude differences are defined as:

$$\Delta u = u_{cu} - u_{\tau}$$

$$\Delta v = v_{cu} - v_{\tau}$$

$$\Delta b = b_{cu} - b_{\tau}$$

$$\Delta y = y_{cu} - y_{\tau}$$

$$\delta Si = \Delta Si_{cu} - \Delta Si_{\tau} .$$

Table 4.2

Observational Results

Date	JD (2440000+)	Phase	Δu	Δv	Δb	Δy	δSi
March 21/22	2493.880	.704	-.304	.472	.632*	.752*	-.003
	.916	.773	-.276*	.471	.613	.701*	-.014
	.950	.838	-.323	.475	.608	.734	-.008
	2494.019	.971	-.300	.496*	.621	.749	-.021
March 23/24	2495.787	.366	-.158	.521	.668	.784	-.005
	.802	.395	-.172	.518	.658	.779	-.007
	.816	.422	-.131*	.510	.644	.773	.012
	.830	.449	-.193	.506	.639	.752	.046
	.862	.510	-.228	.484	.627	.762	.013
	.897	.577	-.266	.468	.617	.751	.007
	.940	.660	-.308	.458	.594	.719*	.002
	.994	.764	-.318	.467	.609	.719	.007
March 24/25	2496.802	.316	-.163	.529	.667	.785	.003
	.843	.394	-.184	.512	.656	.781	.002
	.858	.423	-.204	.500	.638	.765	.006
	.891	.487	-.228	.485	.611*	.747	.002
	.910	.523	-.237	.474	.616	.746	.019
	.945	.590	-.262	.463	.600	.735	.021
	.977	.652	-.277	.465	.603	.735	.017

Table 4.2 (cont'd)

Date	JD (2440000+)	Phase	Δu	Δv	Δb	Δy	δSi
March 28/29	2498.767	.089	-.285	.483	.619	.750	
	.777	.108	-.255	.495	.637	.755	
	.787	.127	-.275	.495	.616	.771*	
	.798	.149	-.273	.496	.638	.764	
	.807	.166	-.250	.490	.581*	.755	
	.819	.175	-.250	.505	.622*	.747	
	.830	.210	-.227	.521	.662	.778*	
	.843	.235	-.232	.509	.642	.773	
March 29/30	2499.748	.974	-.284	.467*	.611	.731	
	.769	.014	-.283	.491*	.617	.734	
	.778	.031	-.273	.477	.613	.752*	
	.804	.081	-.293	.490	.617	.743	
	.813	.099	-.287	.495	.634	.746	
	.821	.114	-.273	.487	.629	.741	
	.829	.129	-.280	.506	.626	.745	
	.839	.148	-.267	.500	.632	.759	
	.857	.183	-.251	.502	.637	.748	
	.866	.200	-.241	.518	.672*	.763	
	.876	.220	-.244	.510	.650	.763	
	.890	.246	-.232	.520	.661	.769	
	.899	.264	-.195	.516	.643*	.767	

It will be noted that silicon observations are available for the first three nights only. A preliminary examination of the data on March 25 showed that the silicon photometry was not providing the data that had been anticipated for reasons discussed in section 4.9 below. For this reason the silicon program was discontinued in favor of a more complete coverage of the light curve in the conventional four colour photometry.

The data in Table 4.2 are plotted in figs. 4.1 through 4.5. Examining these light curves we can see that as would be expected in the oblique rotation theory, the maximum amplitude of light variation is observed in the ultraviolet. The far ultraviolet radiation of deep, hot layers of the star is trapped by the opacity of the abnormally abundant silicon in the star's atmosphere. The atmosphere then reradiates this energy with a wavelength distribution corresponding to its own blackbody temperature, having maximum emission in the near ultraviolet region and decreasing emission at longer wavelengths.

A comparison of these results to those of Hardie (1958) shows that the phase of minimum light has been delayed by about 0.30 P in the 20 years since his observations in 1955. This means that the period is actually longer than the 0.52067 day published by

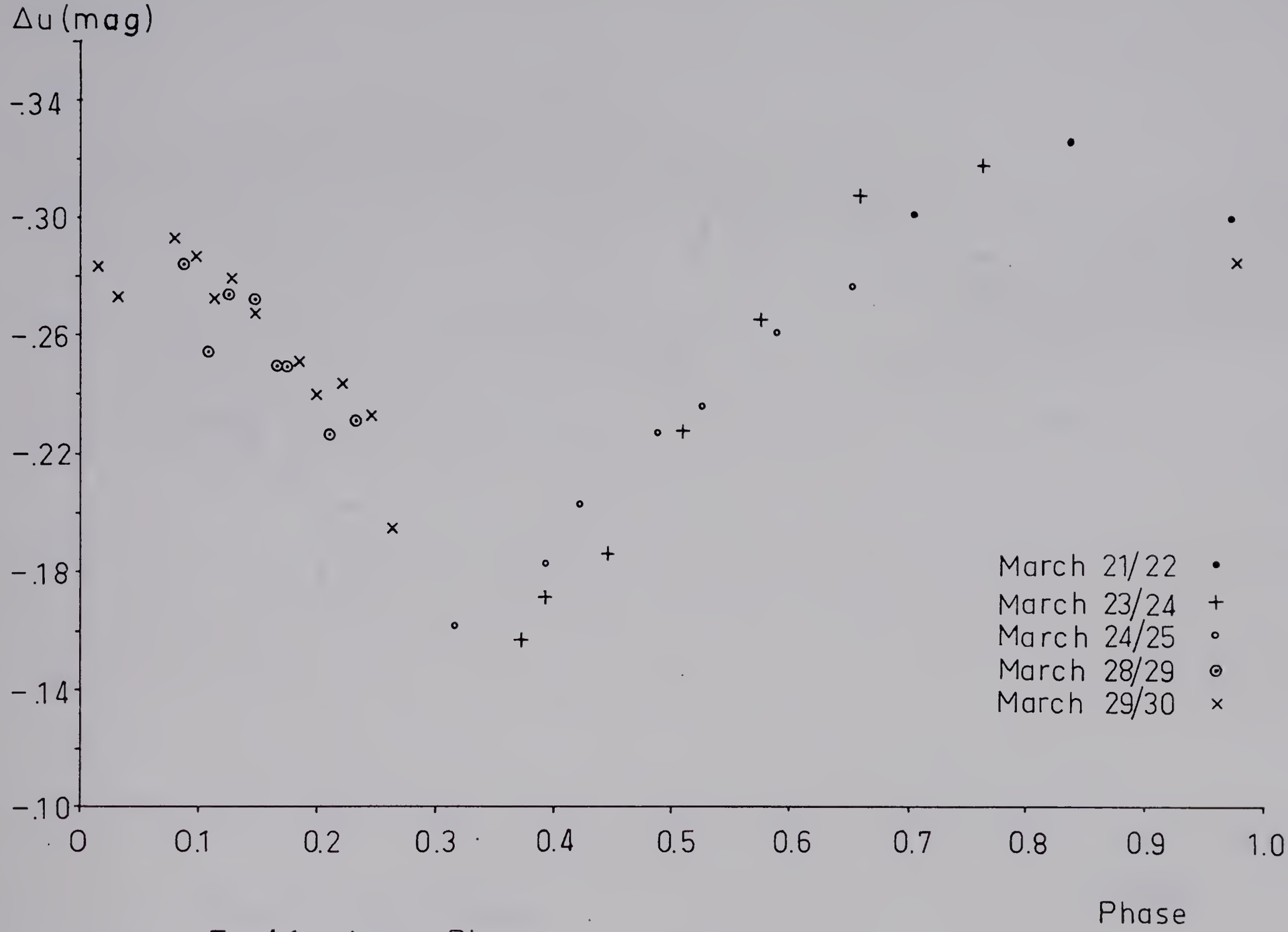

Fig 4-1 Δu vs Phase

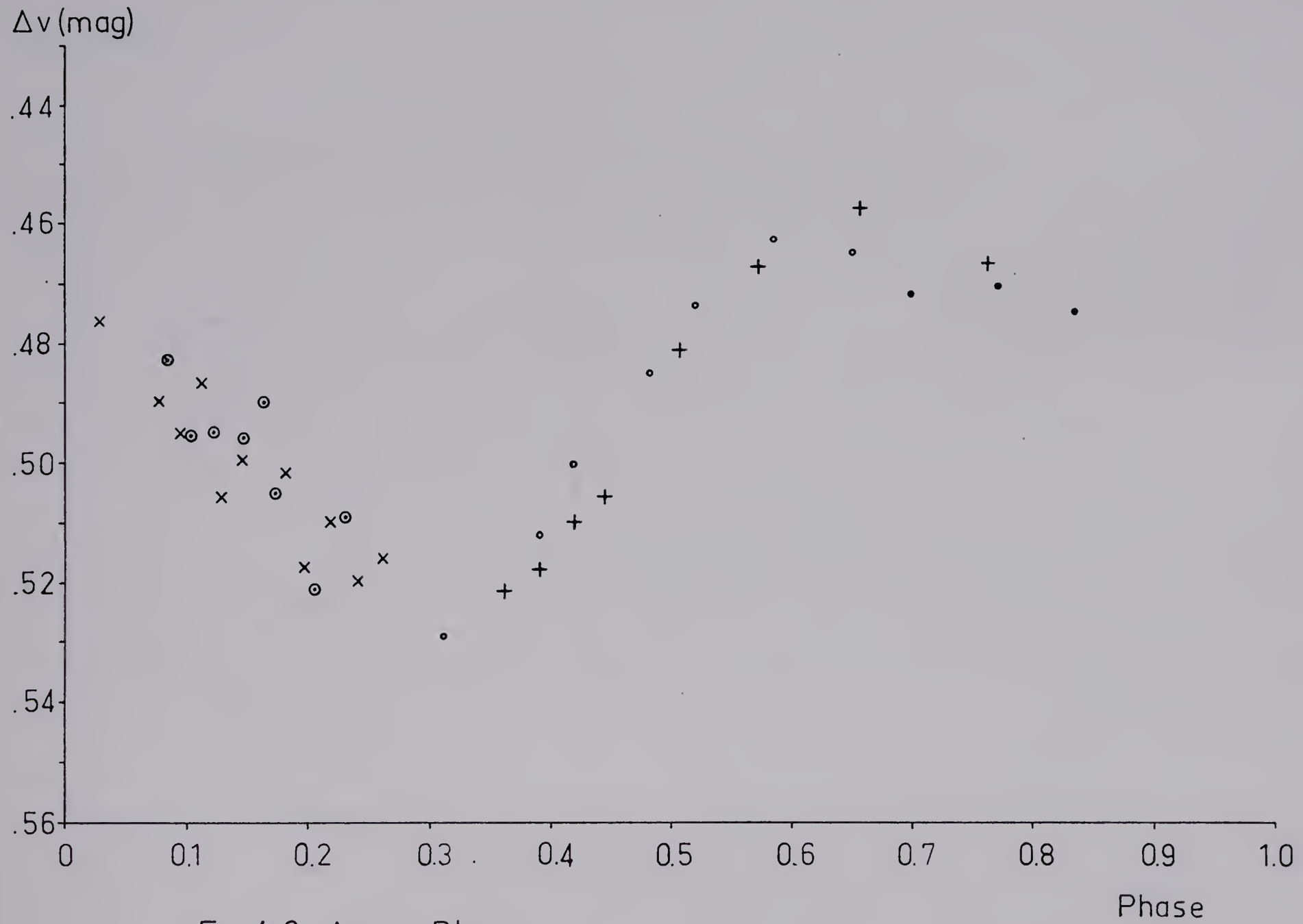

Fig 4-2 Δv vs Phase

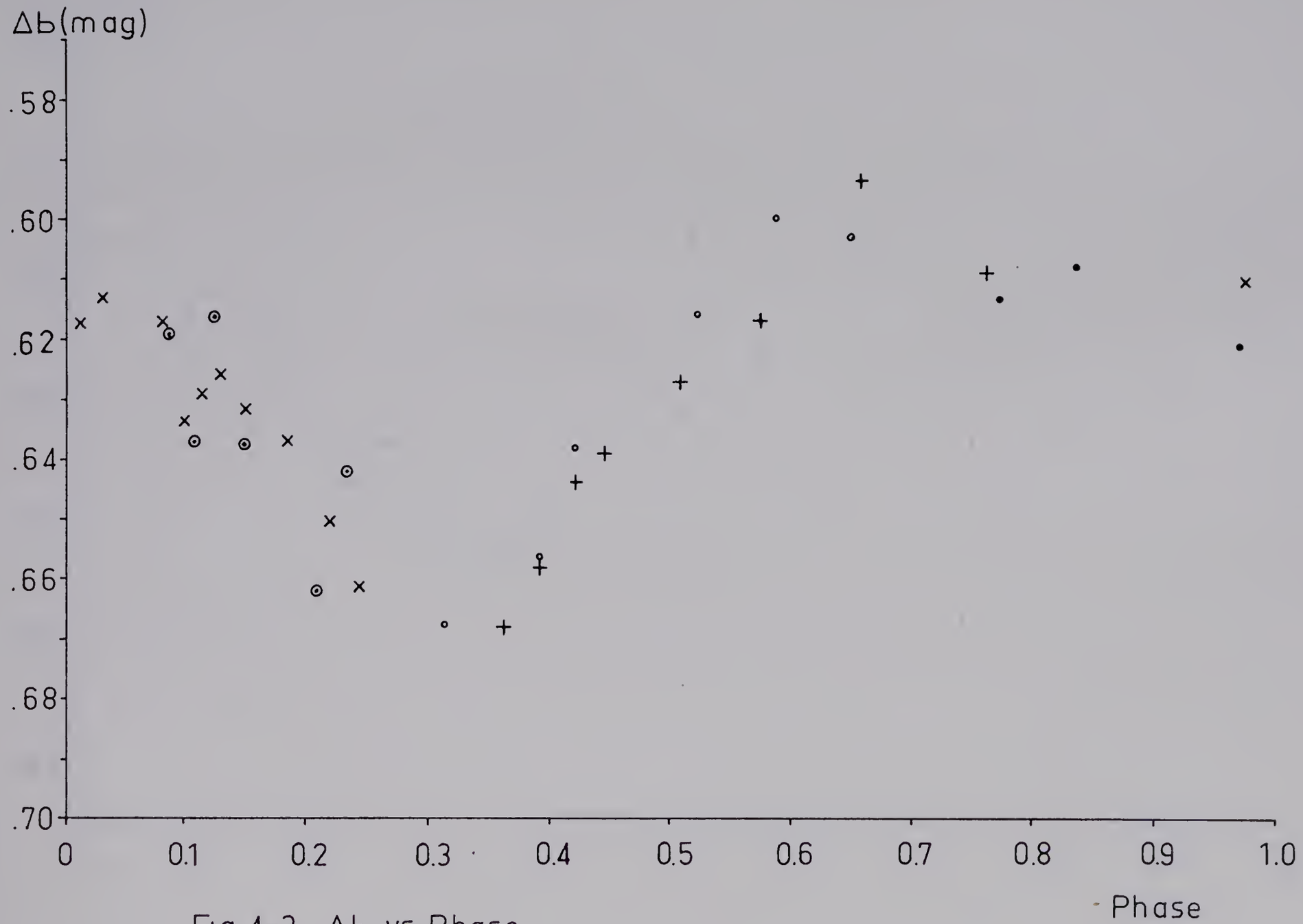

Fig 4-3 Δb vs Phase

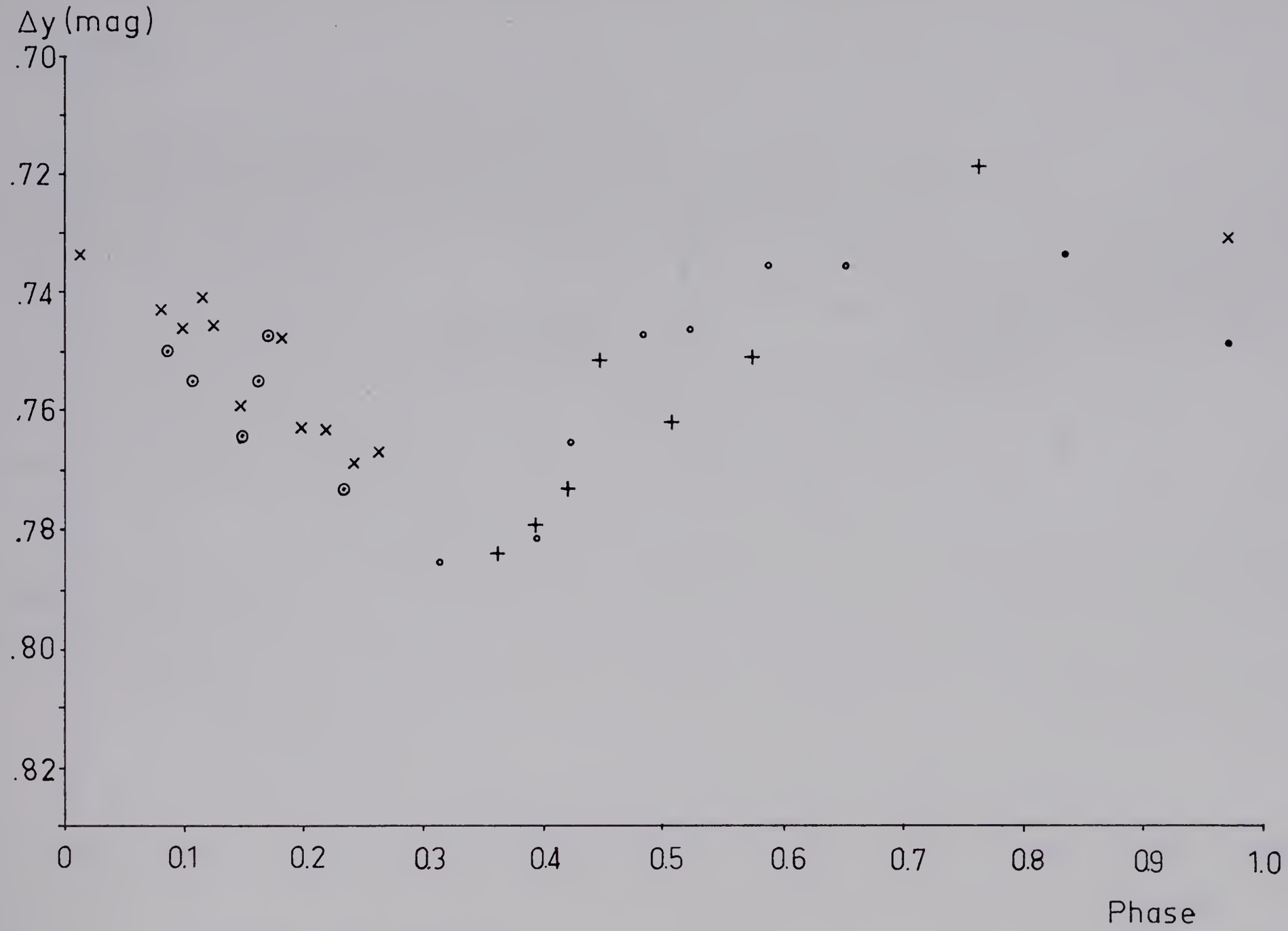

Fig 4-4 Δy vs Phase

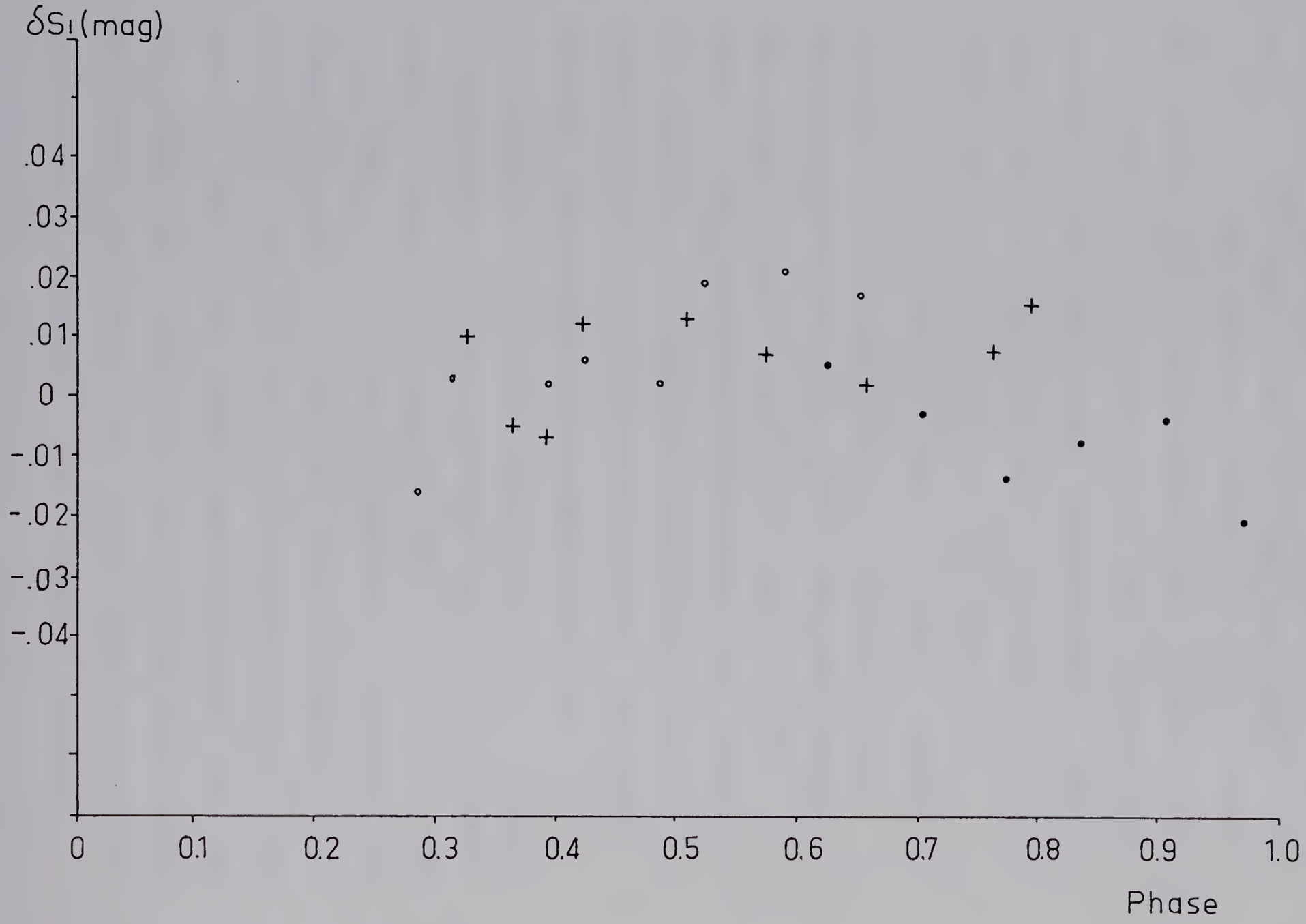

Fig 4-5 δS_1 vs Phase

Deutsch (and used in Hardie's calculations) by about $1.1 \pm 0.2 \times 10^{-5}$ day and should be given as $0.52068 \pm 2 \times 10^{-6}$ day. Observations of this star made by Blanco and Catalano (1971) have yielded a similar correction to Deutsch's value for the period. Other observations by Winzer (1974) show a phase delay of +0.26 P, indicating that the delay found in 1975 is indeed +0.30 P rather than -0.70 P, +1.30 P or some other value.

The four colour photometry data show a scatter of about ±0.005 magnitude with the occasional point deviating from the trend by almost twice this amount. This amount of scatter is somewhat larger than is normal in good differential photometry, but as Table 4.1 shows, the sky conditions during the observing session were below average for this site. The deviation of a few points from the curves by as much as 0.01 magnitude is not surprising in view of the presence of some atmospheric haze and high cirrus clouds on some nights. During their passage in front of the star, these could change the extinction coefficients by amounts large enough to account for deviations from the curves of 0.01 magnitude. The scatter in the observations is noticeably worse on the last two nights, March 28/29 and 29/30. This is probably due to hazy conditions on those nights aggravated by the proximity of the program stars to the Moon, which was full on March 27. This moonlit haze gave fluctuating sky counts as large as 1 or 2 percent of

the signal count, causing an uncertainty in the measured magnitudes as large as 0.01 (2% of a differential magnitude of 0.5).

Certain of the tabulated points are marked with an asterisk (*). These deviate strongly from the trend of the data and have been omitted from the light curves. These points are thought to be the result of procedural errors made during the observations. The most common error of this type is the loss of signal due to part of the disk of the star image being obscured by the diaphragm during the count interval. Since the star images were about 10 arc seconds in diameter and the diaphragm used was only 25 arc seconds across, a relatively small tracking error during the count interval could cause some light loss.

4.9 The Silicon Line Photometry

The results of the silicon photometry are shown in Fig. 4.5. The scatter in these data is twice as large as in the previous curves, since each point represents the difference between two experimentally determined differential magnitudes. The differential silicon index should measure the equivalent widths of the Si II lines at 4128 and 4131 Å, a measure of the apparent abundance of silicon in the star CU VIR. This abundance should be maximum at maximum light according to the oblique rotator model. However, such a maximum is not clearly shown by the data.

The problem here almost certainly lies in the choice of the bandwidth of the narrow filter. In the ideal case, this filter should pass just the wavelengths of the lines in question and none of the undesired continuum. However, a limit is imposed on the minimum usable bandwidth by the lowest acceptable signal level, and as the filter system used here was designed for use with small telescopes, a value of 10 Å FWHM was chosen. Unfortunately, the silicon lines in question are quite narrow. Under the conditions found in the atmospheres of A_p stars, they have equivalent widths of a few tenths of an angstrom each. This means that a change from zero to maximum width of these lines would decrease the signal received through the narrow filter by only a few percent, and the line variation is hidden by the scatter in the data, which is of approximately the same size. From this it seems clear that successful line photometry on narrow spectral features is practical only with telescopes large enough to provide usable signal levels through a filter little wider than the feature of interest.

4.10 Transformations to the Standard uvby Photometric System

An extensive list of observations of standard stars for the uvby system is given by Crawford and

Barnes (1970). The data are given in terms of the colour index (b-y) and the two colour differences $m_1 = (v-b) - (b-y)$ and $c_1 = (u-v) - (v-b)$. In order to calculate the set of transformations that are required to convert the results obtained with a given filter set and photomultiplier to those that would be obtained with Crawford's system, the photometer in question is used to obtain observations of some of the standard stars. The equations which reduce the results of these observations to those obtained with Crawford's system are the necessary transformation equations.

Provided that the spectral characteristics of the filters and photomultiplier used are reasonably similar to those of Crawford's system, the transformations will be linear and have the form:

$$V = y(obs) + A + B(b-y)$$

$$(b-y) = C + D(b-y)(obs)$$

$$m_1 = E + F\, m_1(obs) + J(b-y)$$

$$c_1 = G + H\, c_1(obs) + I(b-y)$$

where (obs) indicates an observed quantity, the remaining magnitude (V), colour index (b-y) and colour differences (m_1,c_1) being those given in Crawford's list of standard stars.

In this case, the observed values were obtained by averaging the results of observing the stars σ Boo (HD 128167) γ Ser (HD 142860), 78 U Ma (HD 113139) and 80 U Ma (HD 116842) on three nights each and the star β Com (HD 114710) on four nights. The average values obtained, and Crawford's standard values for these stars, are shown in Table 4.3.

Table 4.3

Transformation Data

	Observed Values				Standard Values			
Star	(b-y)	m_1	c_1	y	(b-y)	m_1	c_1	V
β Com	-0.892	1.481	-0.379	5.23	0.370	0.191	0.337	4.3
σ Boo	-1.001	1.431	-0.234	5.44	0.253	0.132	0.488	4.5
γ Ser	-0.922	1.396	-0.262	4.79	0.319	0.151	0.401	3.9
78 U Ma	-1.011	1.462	-0.106	5.92	0.244	0.168	0.578	4.9
80 U Ma	-1.145	1.465	+0.175	5.00	0.097	0.192	0.928	4.0

The transformation equations were fitted to these data using the method of least squares. The values of the coefficients A through J which were obtained from this fitting procedure are listed in Table 4.4. These values contain an uncertainty due to calculation and fitting errors of about ±0.05 with the exception of the coefficient I, which is smaller than expected by about 0.5. The definitions of the colour differences imply I = -25, and the rather small scatter

Table 4.4

Transformation Coefficients

Coefficient	Value	Coefficient	Value
A	0.82	F	0.75
B	0.45	G	0.85
C	1.29	H	0.75
D	1.04	I	-0.70
E	-1.08	J	0.08

in the m_1 values means that the coefficient J should be quite accurately determined by the fitting process. In contrast, the c_1 values contain quite large scatter and the I value resulting from the fit is questionable, particularly as only five data points are available. A larger number of observations would probably yield an I value of approximately-0.20.

4.11 Conclusions from the Test Observing Program

The photometer performed very well during the testing program, the mechanical controls proved to be quick and convenient to operate and the optical components also worked satisfactorily. However, the testing program did reveal a need for two minor modifications to the mechanical design, which have subsequently been incorporated into the photometer.

The first of these became necessary when it was discovered that a small amount of light could leak into the photometer at the point where the filter wheel perimeter entered the main body of the instrument. To prevent this, additional metal baffles have been added to improve the light seal in this area.

The second modification is a convenience feature to speed the operation of changing filter wheels. Since the photomultiplier was left uncovered during the wheel change it was necessary to use very subdued lighting during the operation, making it rather slow and awkward. For this reason, a second dark slide has been included between the filter wheel housing and the photomultiplier. This slide is activated by withdrawing the small knob adjacent to the diaphragm viewer (see fig. 4.6). The photomultiplier is covered when the knob is in the out position, and uncovered when the knob is pushed all the way in.

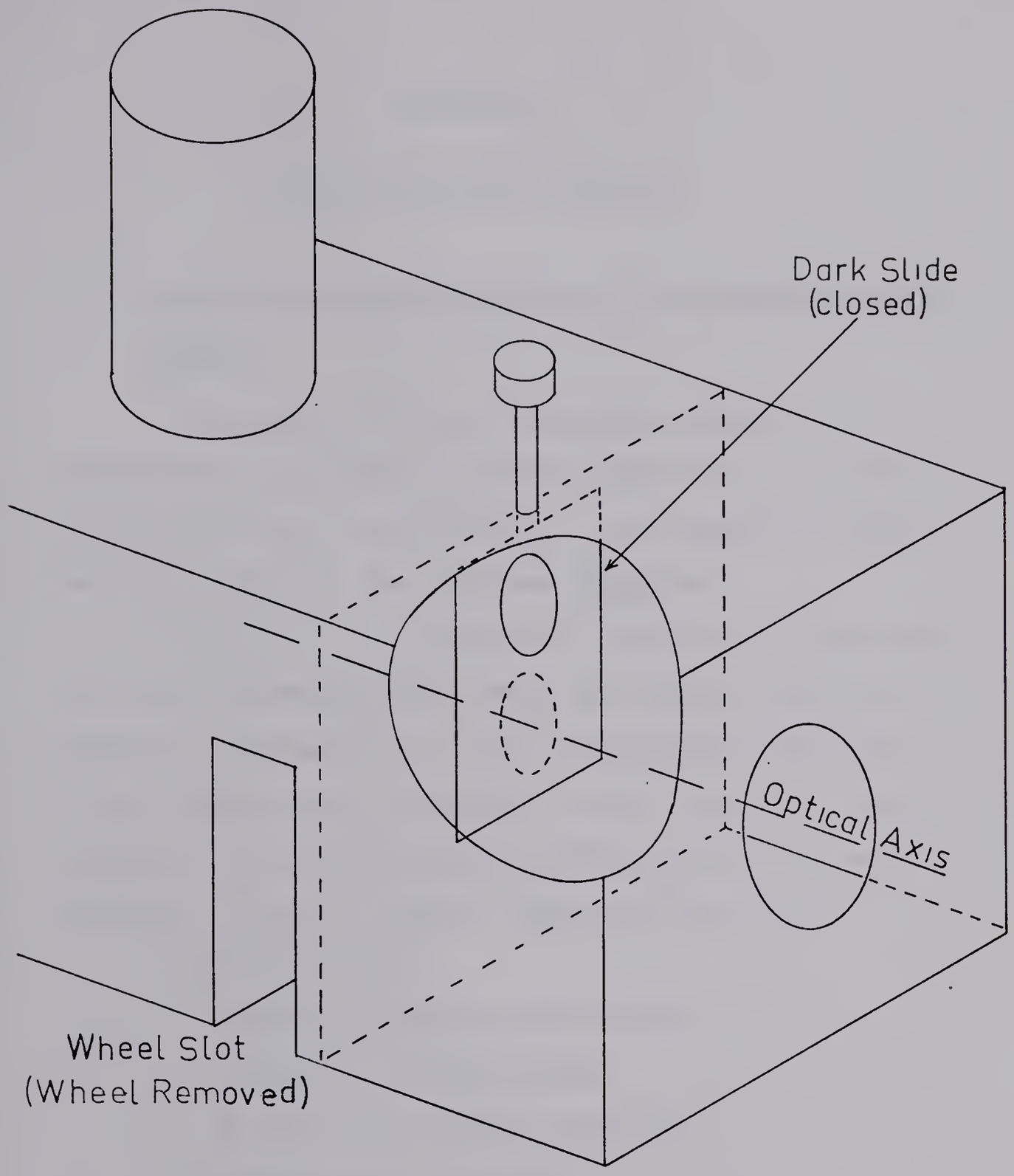

Fig 4-6 Dark Slide for Filter Wheel Change

CHAPTER 5

PHOTON COUNTING PRACTICE

5.1 Optimizing the Performance of the Photon Counting System

The purpose of this concluding chapter is to record for the benefit of future users of the photon counting system those details of its operation which were not given in the previous chapters.

The task of selecting the appropriate values for the many adjustable quantities in a photon counting system is one which at first sounds quite difficult. From a theoretical standpoint, there is a very large number of variables governing the operation of such a system. A list of some of these is given below:

Photomultiplier:

- spectral response of cathode
- cathode to anode voltage
- output pulse height spectrum
- output pulse duration
- pulse transit time

Amplifier:

- input impedance (resistive and capacitive)
- risetime and bandwidth
- gain

Discriminator

bandwidth and "deadtime"

threshold voltages (upper and lower)

Count intervals for both signal and noise

Spectral bandwidths of filters

Black body temperature of light source.

In a theoretical photon counting system, all of these quantities are variable, making the process of optimizing such a generalized system rather difficult. The approach used in this general case is discussed by Sedmak (1972). Fortunately, in practice the optimization process is somewhat simplified by limitations that are imposed on the values of certain variables. The photomultiplier pulse width, and the bandwidths of the amplifier and discriminator are limited by the technologies involved in their construction. Once a photomultiplier has been chosen (for reasons discussed in Chapter 3) and the restriction of the use of standard photometric filters is applied, the number of variables has been reduced to four. These are the cathode to anode voltage, amplifier gain, discriminator threshold voltage, and count interval duration. The optimum values of the first two of these are fixed by the behaviour of photomultiplier count rates as functions of the cathode to anode voltage. As described in Chapter 1, photon counting photometry requires an

overall gain of the order of 10^9. To achieve this gain while maintaining long term stability of performance most photomultipliers require external signal amplification of the order of 10^3. When used with such an amplifier and a moderate discriminator threshold voltage (around 300 mv), the count rates produced by the noise and the signal from a constant light source have the general behaviour shown by fig. 5.1.

For an EMI 9502S tube, the knee regions of the curves occur at approximately 1200 volts. A voltage higher than this must be used to place the tube on the flat plateau region of the curves. Operation on the plateau region is necessary to ensure reproducibility of the results over long time periods, in spite of aging effects in the high voltage supply and the voltage dividing resistors. However, as the voltage is increased beyond this value, the signal to noise ratio decreases because the noise increases with voltage somewhat faster than the signal.

The optimum operating voltage for a tube used in photon counting is thus the voltage which places it at the left edge of the plateau region in fig. 5.1. For an EMI 9502S this is about 1300 volts.

To produce a satisfactory plateau of the above type in the present system requires an amplifier gain of 2000. Since the preamplifier has a gain of 10, the

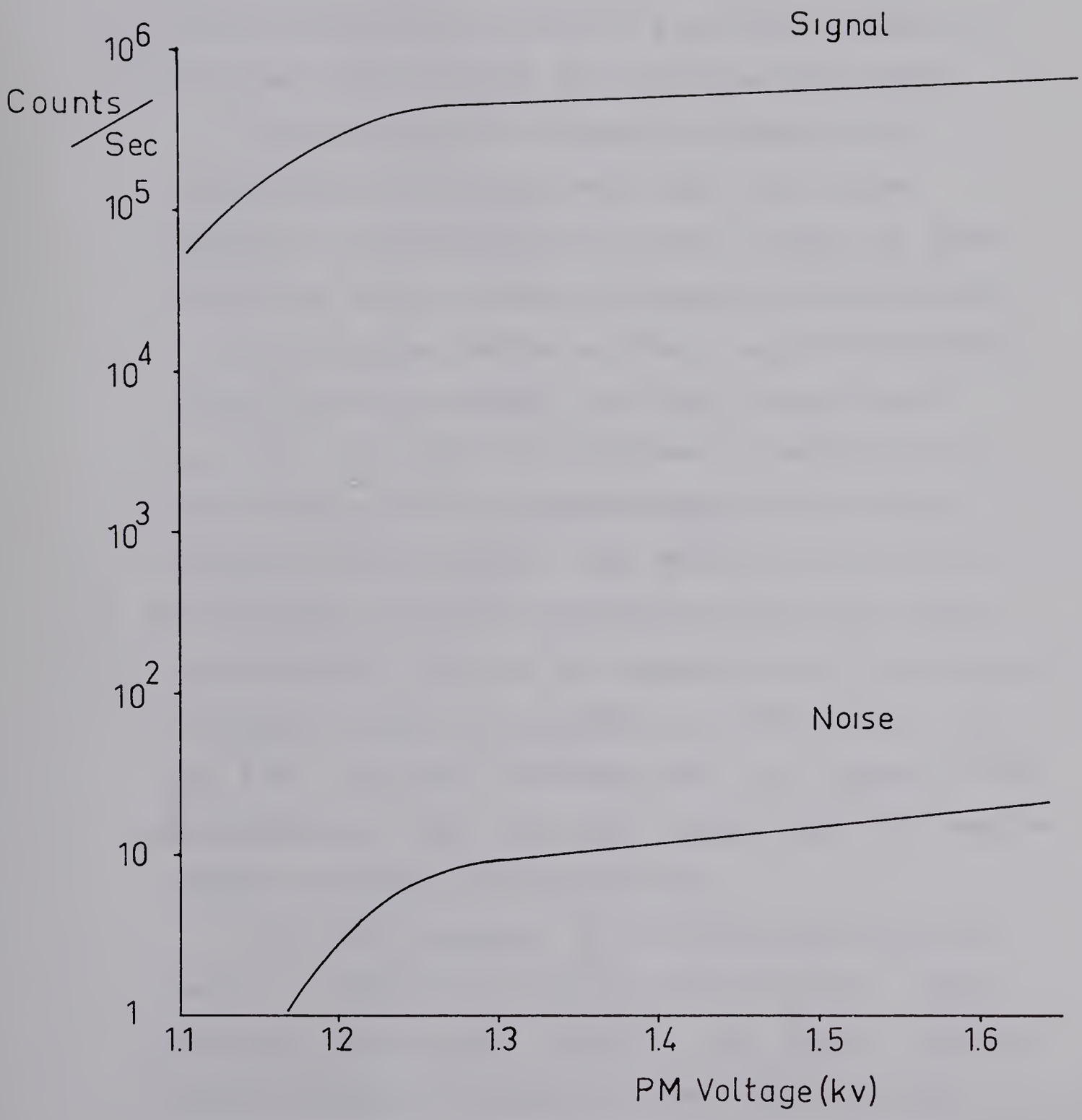

Fig 5-1 Output of EMI9502S Photomultiplier

spectroscopy amplifier should be set to a gain of 200. While still higher gain values could be employed if required, the use of ultrahigh amplifier gains (>10,000) should be avoided or a serious increase in the noise susceptibility of the system will result.

The discriminator threshold voltage should theoretically be adjusted until only the largest pulses in the photomultiplier output, which are those originating at the cathode, trigger the discriminator. All smaller pulses, which are due to spurious electron emission from the dynodes, are thus excluded (see fig. 5.2). In reality the picture is complicated by the overlapping of the distributions of the cathode and dynode pulse heights. The choice of the correct discriminator threshold involves plotting the overall signal to noise ratio of the system against discriminator threshold voltage and choosing the maximum point (see fig. 5.3). The best threshold level will depend on the photomultiplier tube involved; a noisy tube will require a higher threshold than a quiet one.

The final parameter in the photon counting process is the duration of the counting interval. This has only a second order effect on the results, but can become important with the low count rates obtained from faint stars. Since the arrival of photons at the cathode is governed by Poisson statistics, the

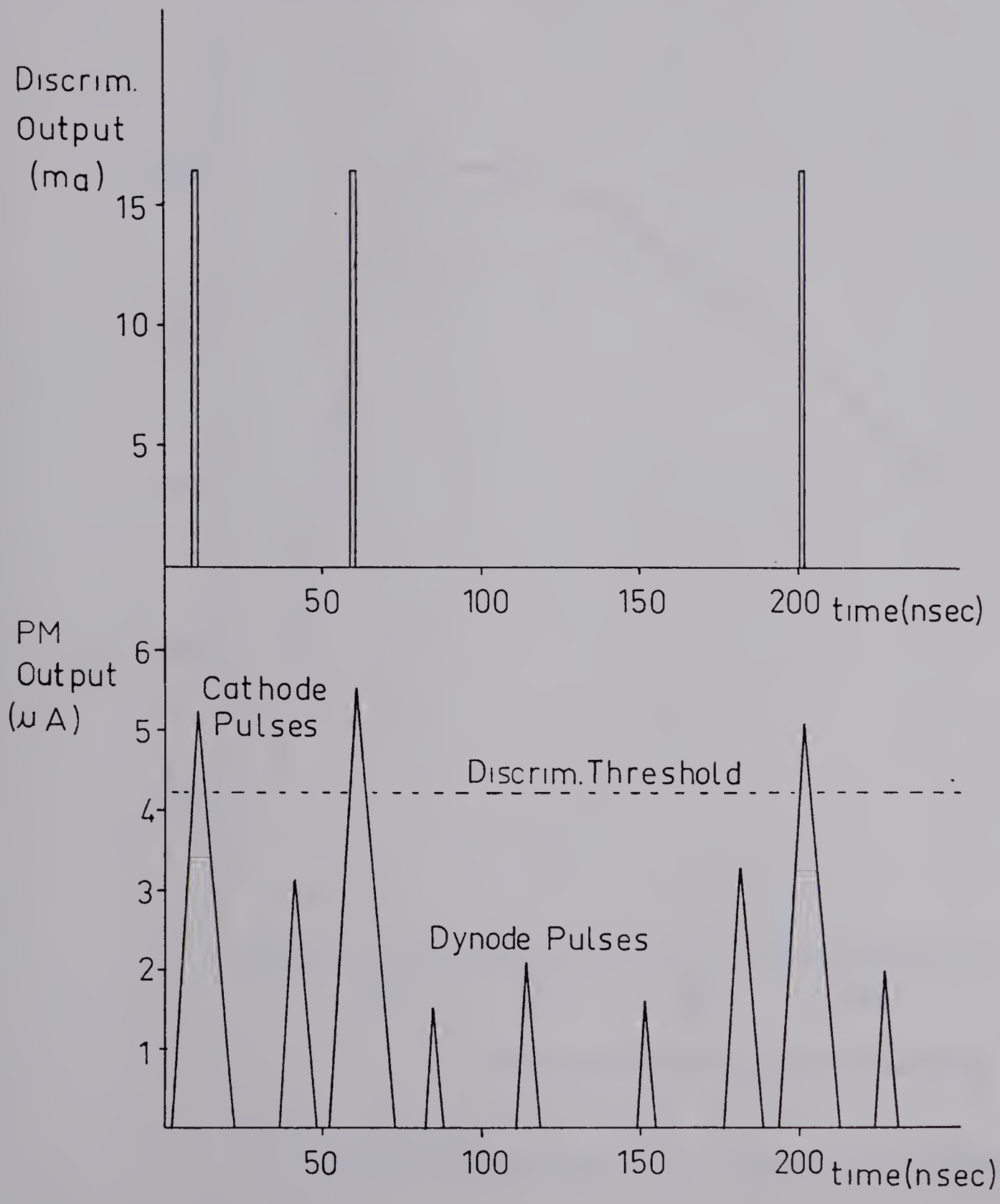

Fig 5-2 The Pulse Discrimination Process

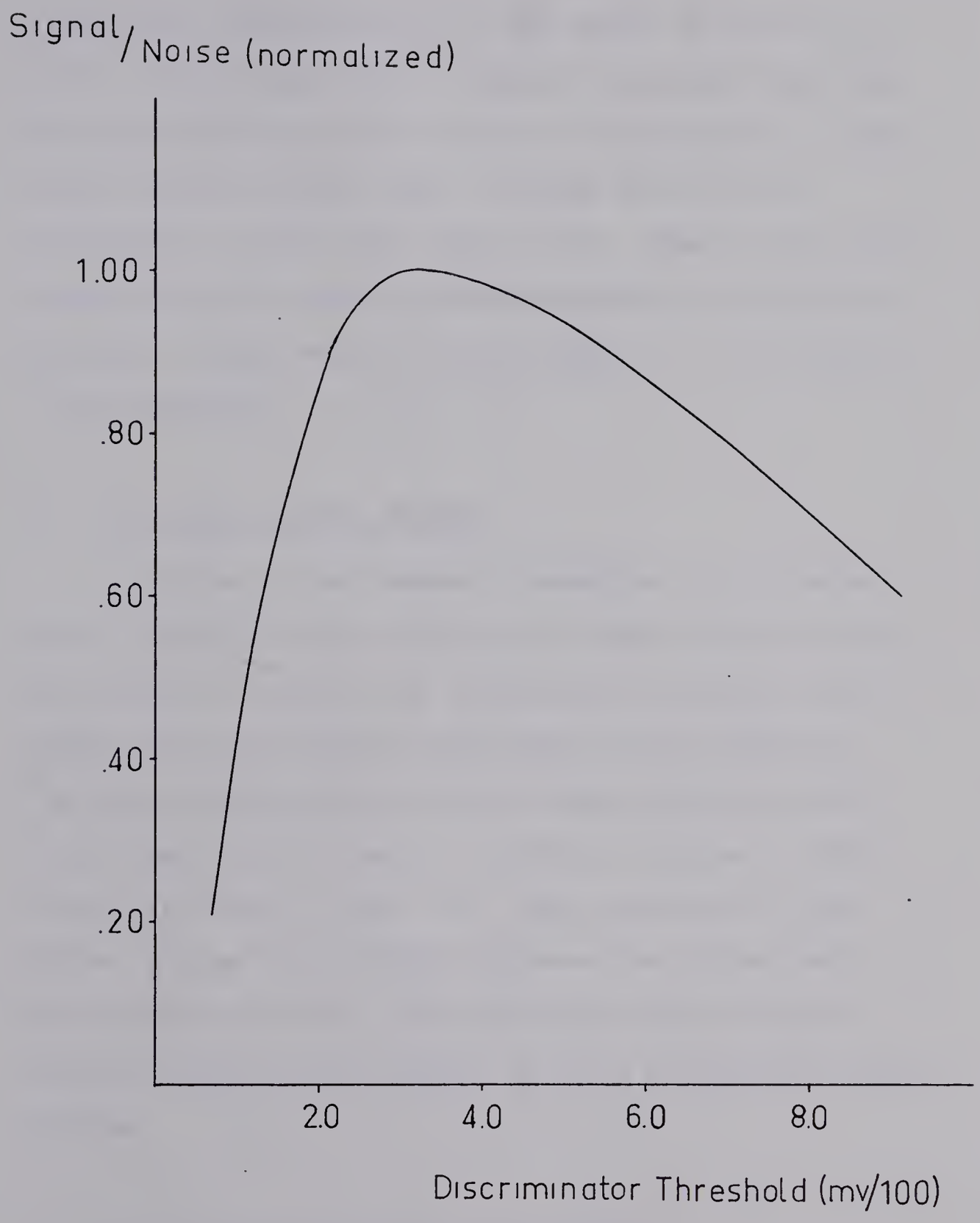

Fig 5-3 Optimizing Discriminator Threshold

fractional standard error in any count of total n is $(n)^{-\frac{1}{2}}$. This means that to reduce the uncertainty due to the randomness of the arrival of the photons, large total counts must be used. A count of 10,000 is necessary to limit this error to 1%. Thus at low count rates the count interval duration must be increased to maintain a total count of this order if 1% accuracy is to be retained.

5.2 The High Voltage Filter

Because of the dramatic reduction in the noise count produced at Kitt Peak by the high voltage filter mentioned in section 4.4, a similar filter was introduced into the output of the high voltage supply at the Devon Observatory to see if any reduction in the noise count would result. A circuit diagram of this filter is shown in fig. 5.4. The inclusion of this filter did not appreciably decrease the noise count of the Devon system, indicating that noise induced from the high voltage supply is not a problem with this system.

5.3 Future Improvement of the System

A program of test observations has shown that in its present state the photon counting system will

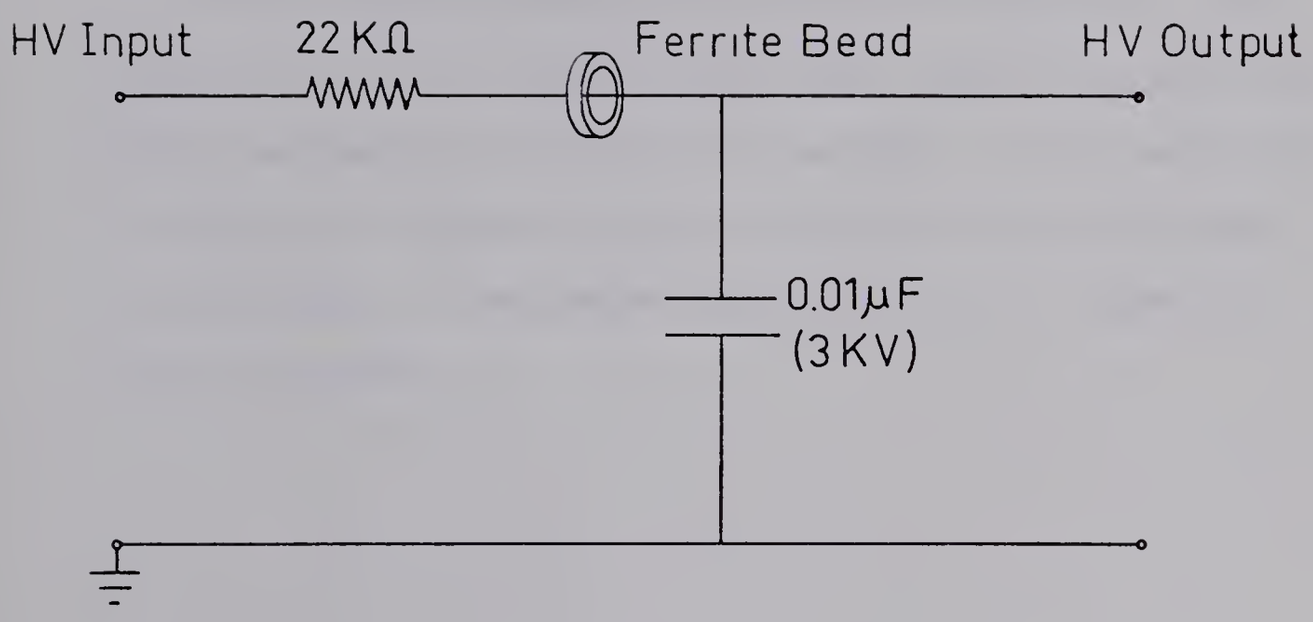

Fig 5-4 The High Voltage Filter

provide signal to noise ratios of the order of 100 when used to observe stars of the ninth magnitude with intermediate band filters. A further increase in the signal to noise ratio of the system (of at least a factor of 10) may be obtained by cooling the photomultiplier to reduce thermal electron emission. It is suggested that the present photomultiplier housing be modified by the inclusion of a dry ice cooled jacket and the appropriate heater mechanism for the quartz window. It is desirable to retain the present housing because of its excellent RF shielding, an important consideration in a photon counting system.

APPENDIX 1

The contents of this section describe the procedure for operating the photon counting system. The settings of all Ortec module controls necessary for normal operation of the system have been recorded for future reference.

Four separate switches must be operated to supply AC power to the entire system. These are located on the printer, the Ortec rack power supply, the remote display box and the high voltage supply. The digital clock mounted inside the printer chassis is connected directly to the power line and is on whenever the printer is plugged in. The remote control box and the pulse preamplifier are located in the observatory, but both receive their power from the Ortec rack. The printer interface also draws its power from the Ortec rack, so all of these devices plus the four Ortec modules are turned on by the rack power switch.

To operate the high voltage supply, turn on the AC power, dial the correct voltage (usually 1300 V) on the voltage thumbwheels, and turn the current limit knob clockwise until the current meter needle is steady. When switching off the high voltage, both the current and voltage must be set to zero before the AC power is switched off, or the power left in the output capacitors will blow the 5 A fuse. The high voltage should

be switched on at least an hour before the start of observing to allow the tube time to stabilize.

The digital clock should be set to the radio time signal (WWV at 2.5, 5 or 10 MHz) before each observing session. To do this, move the toggle switch to the "stop" position and use the recessed pushbuttons to set the hours, minutes and seconds to an upcoming time. When this time is announced on the radio, move the toggle switch to the "run" position.

The required settings for all the Ortec module controls are given below:

Spectroscopy Amplifier

- Input switch to positive
- Output switch to positive
- Coarse gain to 200
- Fine gain knob to 1.0

Discriminator

- Reset switch to prompt
- Discriminator level knob to 3.0

Timer

- Time base to 0.1 sec
- Preset knob to 1
- Multiplier to 100 (Gives 10 sec count)

Counter

- Count-stop switch to count
- Master-slave switch to master

APPENDIX 2

The Unreduced Data

The table below presents the observational data without the conversion to magnitudes or the corrections for extinction effects. For March 21/22 (JD 2442493.870 to 2442494.019) each value represents the average of 5 10 second integrations. The reduction to magnitudes of all values except those marked with a * requires the subtraction of a scale factor of 2.504 from the magnitudes derived from the tables. This factor arises from a scale change required by the current integrator under strong signal conditions. For the remaining nights, the value shown is the average of 5 10 second counts with the sky count subtracted. For easier computation, the actual counts were divided by 100 to produce the counts shown below.

Table A2.1

The Unreduced Data

Star	JD (2440000+)	Air Mass	COUNT					
			u	v	b	y	Si W	Si N
τ	2493.870	1.169	1044	2745	3998	1462	1836	874*
CU	" .880	1.155	1370	1784	2243	734*	1121	535*
τ	" .906	1.157	1043	2738	4016	1461	1842	868*
CU	" .916	1.149	1402	1778	2286	744*	1154	542*
τ	" .940	1.202	995*	2657	3876	1420	1773	831*
CU	" .950	1.195	1334	1719	2218	723*	1112	525*
τ	2494.011	1.538	819*	2375	3523	1333	1596	749*
CU	" .019	1.515	1065	1512	1998	671*	973*	465*
CU	2495.787	1.468	5083	7566	9745	3187	5017	240
τ	" .796	1.390	4581	12578	18422	6633	8580	409
CU	" .802	1.380	5464	7900	10133	3256	5183	247
τ	" .809	1.320	4814	13006	18778	6735	8779	416
CU	" .816	1.308	5497	8139	10360	3319	5377	253
τ	" .823	1.265	4984	13224	18971	6809	8951	426
CU	" .830	1.247	6067	8331	10527	3352	5408	256
τ	" .837	1.218	5102	13329	19022	6691	8699	427
CU	" .862	1.172	6540	8781	10910	3434	5706	270
τ	" .870	1.163	5327	13755	19500	6933	9269	444
CU	" .897	1.145	6873	9015	11152	3494	5793	273
τ	" .905	1.161	5337	13807	19586	6954	9298	441
CU	" .940	1.187	6904	8960	11229	3521	5786	273
τ	" .947	1.232	5076	13443	19158	6788	9033	427
CU	" .994	1.392	6305	8507	10823	3455	5471	257
τ	2496.002	1.510	4416	12518	18364	6641	8416	398
τ	2496.794	1.383	5015	13495	19320	7119	8832	434
CU	" .802	1.366	5879	8332	10477	3477	5335	264
τ	" .837	1.214	5484	14142	19838	7303	9285	456
CU	" .843	1.203	6536	8844	10856	3663	5606	275

Table A2.1 (cont'd)

The Unreduced Data

Star	J.D. (2440000+)	Air Mass	COUNT u	v	b	y	Si W	Si N
τ	" .851	1.184	5558	14222	19937	7318	9341	460
CU	" .858	1.175	6736	8992	11100	3625	5717	280
τ	" .883	1.155	5663	14446	20076	7334	9412	462
CU	" .891	1.145	7021	9271	11346	3691	5865	285
τ	" .902	1.160	5627	14302	19978	7311	9330	462
CU	" .910	1.150	7035	9250	11345	3686	5854	285
τ	" .937	1.218	5509	14184	19876	7292	9296	457
CU	" .945	1.205	7062	9287	11460	3716	5867	283
τ	" .968	1.320	5220	13792	19520	7195	8987	442
CU	" .977	1.316	6762	8996	11214	3661	5653	274
τ	2498.763	1.510	3962	10941	16263	5971		
CU	" .767	1.516	5129	6993	9176	2988		
τ	" .772	1.447	4131	11148	16454	6000		
CU	" .777	1.442	5231	7065	9145	2993		
τ	" .782	1.380	4199	11240	16341	6028		
CU	" .787	1.380	5403	7124	9261	3013		
τ	" .792	1.332	4293	11316	16671	6092		
CU	" .798	1.332	5528	7171	9262	3015		
τ	" .802	1.290	4468	11551	16807	6085		
CU	" .807	1.290	5630	7352	9366	3036		
τ	" .812	1.254	4661	11935	16955	6150		
CU	" .819	1.243	5894	7525	9585	3095		
τ	" .823	1.220	4708	12092	17458	6291		
CU	" .830	1.210	5839	7509	9505	3078		
τ	" .837	1.190	4835	12131	17405	6302		
CU	" .843	1.180	6015	7613	9655	3100		
τ	2499.741	1.691	3519	10180	15716	5715		
CU	" .748	1.708	4623	6570	8910	2906		
τ	" .764	1.487	4006	10887	16323	5882		

Table A2.1 (cont'd)

The Unreduced Data

Star	JD (2440000+)	Air Mass	COUNT u	v	b	y	Si W	Si N
CU	" .769	1.490	5216	6920	9238	2990		
τ	" .774	1.426	4059	10992	16402	5962		
CU	" .778	1.422	5374	7081	9322	2980		
τ	" .799	1.290	4625	11894	17443	6186		
CU	" .804	1.290	6051	7572	9883	3123		
τ	" .808	1.252	4718	12072	17603	6237		
CU	" .813	1.254	6130	7655	9825	3139		
τ	" .816	1.225	4770	12009	17501	6183		
CU	" .821	1.230	6129	7664	9808	3125		
τ	" .825	1.209	4800	12110	17548	6231		
CU	" .829	1.203	6208	7717	9872	3137		
τ	" .834	1.190	4896	12288	17718	6284		
CU	" .839	1.184	6238	7767	9907	3128		
τ	" .852	1.164	4973	12348	17719	6249		
CU	" .857	1.160	6234	7805	9871	3146		
τ	" .862	1.153	5025	12509	17910	6303		
CU	" .866	1.149	6240	7792	9630	3128		
τ	" .871	1.155	4976	12321	17692	6265		
CU	" .876	1.145	6190	7742	9746	3107		
τ	" .885	1.158	4951	12265	17788	6262		
CU	" .890	1.148	6092	7638	9699	3090		
τ	" .894	1.166	5089	12245	17574	6247		
CU	" .899	1.153	6052	7655	9752	3089		

BIBLIOGRAPHY

Babcock, H.W. (1947) Astrophysical Journal 105, 105.

Babcock, H.W. (1958) Astrophysical Journal Suppl. Ser. 3, 141.

Blanco, C. and Catalano, F.A. (1971) Astronomical Journal 76, 630.

Brown, B. (1968) Photoelectric Observations, M.Sc. Thesis, U. of A.

Crawford, D.L. and Barnes, J.V. (1970) Astronomical Journal 75, 978.

Deutsch, A.J. (1947) Astrophysical Journal 105, 283.

Deutsch, A.J. (1952) Astrophysical Journal 116, 536.

Deutsch, A.J. (1956) Publ. Astron. Soc. Pacific. 68, 92.

Evans, R.D. (1955) The Atomic Nucleus (New York: McGraw-Hill).

Hardie, R.H. (1958) Astrophysical Journal 127, 620.

Hardie, R.H. (1962) Astronomical Techniques, ed. by W.A. Hiltner (U. of Chicago Press, Chicago) p.178.

Johnson, H.L. and Morgan, W.W. (1953) Astrophysical Journal 117, 313.

Michaud, G. (1970) Astrophysical Journal 160, 641.

Sedmak, G. (1972) Astronomy and Astrophysics 18, 232.

Stebbins, J. (1907) Astrophysical Journal 26, 326.

Stromgren, B. (1963) Basic Astronomical Data, ed. by K.A. Strand (U. of Chicago Press, Chicago) p.123.

Tomaszewski, L. (L974) A Photometric Study of El Cephei, M.Sc. Thesis, U. of A.

Winzer, J.E. (1974) The Photometric Variability of the Peculiar A Stars, Ph.D. Thesis, U. of Toronto.